First posted online on 13 October 2020 as 10.1242/dev.195578
Access the most recent version at http://dev.biologists.org/lookup/doi/10.1242/dev.195578

PLP-1 is essential for germ cell development and germline gene silencing in *C. elegans*

Rajaram Vishnupriya[1], Linitha Thomas[2], Lamia Wahba[3, 4], Andrew Fire[3, 4] and Kuppuswamy Subramaniam[1,*]

[1]Department of Biotechnology, Indian Institute of Technology–Madras, Chennai 600036, India
[2]Department of Biological Sciences & Bioengineering, Indian Institute of Technology, Kanpur 208016, India
[3]Department of Pathology, Stanford University School of Medicine, Stanford, California, USA
[4]Department of Genetics, Stanford University School of Medicine, Stanford, California, USA

[*]Author for correspondence:
K. Subramaniam
Email: subbu@iitm.ac.in
Phone: 91-44-22574119
Department of Biotechnology
Indian Institute of Technology–Madras
Chennai 600036
India

KEY WORDS: Purα; *puf-8*; P granules; piRNA; major sperm proteins

Abstract

The germ line genome is guarded against invading foreign genetic elements by small RNA-dependent gene-silencing pathways. Components of these pathways localize to, or form distinct aggregates in the vicinity of, germ granules. These components and their dynamics in and out of granules are currently being intensively studied. Here, we report the identification of PLP-1, a *C. elegans* protein related to the human single-stranded nucleic acid-binding protein called Pur-alpha, as a component of germ granules in *C. elegans*. We show that PLP-1 is essential for silencing different types of transgenes in the germ line, and for suppressing the expression of several endogenous genes controlled by the germline gene-silencing pathways. Our results reveal that PLP-1 functions downstream of small RNA biogenesis during initiation of gene silencing. Based on these results and the earlier findings that Pur-alpha proteins interact with both RNA and protein, we propose PLP-1 couples certain RNAs with their protein partners in the silencing complex. Its orthologs localized on RNA granules may similarly contribute to germline gene silencing in other organisms.

INTRODUCTION

Maintenance of germline genome integrity is crucial for faithful genetic inheritance across generations. This task is accomplished by germline-specific genome surveillance mechanisms that recognize "self" and "non-self" nucleic acid sequences. These mechanisms protect the expression of endogenous genes that normally function in the germ line, but can silence the expression of foreign genetic elements, including artificially-introduced transgenes, and restrict the expression of certain endogenous loci in the germ line.

Silencing of some transposons, transgenes, certain endogenous loci, and the sequence-specific silencing triggered by experimentally-introduced dsRNA (RNAi) all involve three major steps: generation of primary small interfering RNAs (primary siRNAs); amplification of the initial signal, which involves the production of secondary siRNAs in many organisms; and systemic disruption of target expression by cleavage of the target RNA, although other modes of regulation are also employed [for a review see (Billi et al., 2014)]. The different silencing pathways rely on distinct proteins, but also share certain components, particularly in the latter steps. For example, in *Caenorhabditis elegans*, the *mutator* proteins are essential for transposon silencing and contribute to the RNAi response (Ketting et al., 1999; Phillips et al., 2012). In the RNAi pathway, exogenous dsRNAs are cleaved by the ribonuclease Dicer into primary siRNAs, which then associate with and guide the Argonaute (AGO) protein RDE-1 to target sequences (Bernstein et al., 2001; Ketting et al., 2001; Parrish and Fire, 2001; Yigit et al., 2006). Whereas, in the pathway that silences transgenes and endogenous genes, endogenously-encoded small RNAs, called piRNAs, guide the Piwi AGO protein PRG-1 to target sequences (Bagijn et al., 2012; Lee et al., 2012).

Once at the target, the primary siRNA-AGO complex recruits the RNA-dependent RNA polymerase (RdRP) system, which generates secondary siRNAs using the target sequence as template (Pak and Fire, 2007; Sijen et al., 2001). In *C. elegans*, many of the secondary siRNAs are 22-nucleotides (nt) long and contain a triphosphorylated G at the 5′ end (22G-RNAs) (Gent et al., 2010; Pak and Fire, 2007). The 22G-RNAs associate with either a distinct AGO, CSR-1, or one of 12 worm-specific AGOs (called WAGOs) which guide small RNAs to target sequences (Gerson-Gurwitz et al., 2016; Gu et al., 2009; Guang et al., 2008). Besides AGOs, several

proteins aid RdRP recruitment. These include the Dicer-related RNA helicase DRH-3 and the Tudor proteins ERI-5 and EKL-1 (Gu et al., 2009; Thivierge et al., 2011). In addition, the *mutator* proteins MUT-2/RDE-3, MUT-7 and MUT-16 also apparently participate directly or indirectly in the biogenesis / stability of 22G-RNAs (Phillips et al., 2012). MUT-2/RDE-3 is a ribonucleotidyltransferase that adds pUG repeats to the targets. The pUG tails not only facilitate RdRP recruitment, but convert such pUG-tailed RNAs into templates for RdRPs (Shukla et al., 2020).

Many proteins mentioned above have been observed to localize to germ granules (Batista et al., 2008; Claycomb et al., 2009; Conine et al., 2010; Gu et al., 2009). These granules, known as P granules in *C. elegans*, are aggregates of RNAs and proteins (Eddy, 1975; Strome and Wood, 1982). P granules, like the other RNA granules, are biomolecular condensates having physical properties characteristic of liquid droplets (Brangwynne et al., 2009). Their components are important in the transport, stability and translational regulation of certain germline mRNAs, and organize gene-silencing pathways in the germ line (Dodson and Kennedy, 2019; Lev et al., 2019; Sheth et al., 2010; Spike et al., 2008; Updike and Strome, 2010; Voronina and Seydoux, 2010). Recent findings reveal distinct subregions adjacent to where the core P granule components such as PGL-1 localize. It emerges that the components in these subregions have distinct functions, and assemble independently of the core P granule components. For example, the *mutator* proteins, nucleated by MUT-16, form distinct foci adjacent to P granules. The formation and stability of these *Mutator* foci do not require the known P granule components (Phillips et al., 2012). Similarly, ZNFX-1, which functions in the transgene-silencing pathway, and WAGO-4 form distinct liquid-like condensates, called Z granules, sandwiched between P granules and *Mutator* foci (Ismhidate et al., 2018; Wan et al., 2018). What other components, if any, are present in these structures, and how the various components coalesce into physically and functionally distinct subregions are poorly understood. Importantly, how being part of such assemblies helps the individual components to function in gene silencing is not clear.

Here, we identify PLP-1 (Pur-alpha-like protein), the *C. elegans* ortholog of the conserved Pur-alpha proteins, as a new component of the germline gene-silencing machinery. PLP-1 localizes to P granules, and its loss causes temperature-sensitive sterility. Our experiments reveal a role for PLP-1 in silencing transgenes, repetitive DNA arrays and piRNA sensors, and

for robust RNAi response. Furthermore, we find that PLP-1 modulates the expression of several germline-enriched genes that have been earlier shown to be controlled by the silencing pathways.

RESULTS

Simultaneous loss of PLP-1 and PUF-8 disrupts oogenesis

The conserved RNA-binding protein PUF-8 is a key regulator of germ cell development in *C. elegans*. However, even null alleles of *puf-8* cause only temperature-sensitive sterility (Subramaniam and Seydoux, 2003). Exploiting this feature, earlier work in our laboratory had isolated a number of mutant alleles that displayed constitutive sterility when in double mutant combination with the *puf-8* mutation (Maheshwari et al., 2016; Vaid et al., 2013). While mapping one such new mutant allele, we discovered that the RNAi-mediated depletion of PLP-1 (Pur-alpha Like Protein-1), which shares sequence similarity with the human protein Pur-alpha (Purine-rich element binding protein-alpha) (Bergemann et al., 1992), made *puf-8(-)* worms sterile at 20°C, at which they were otherwise fertile. To examine this sterility phenotype further, we used the *ok2155* allele of *plp-1*, which is an 1107-bp deletion that deletes the first two exons and part of the promoter region, and constructed a *puf-8(ok302); plp-1(ok2155)* double mutant strain (hereafter referred to as *puf-8; plp-1*) and examined the germ line systematically (Table S1). When raised at 20°C, all the *puf-8* and *plp-1* single mutants were fertile (n = 548 and 500, respectively). By contrast, about 99 % of the *puf-8; plp-1* double mutants were sterile (n = 358), which reveals a potential redundancy between *puf-8* and *plp-1* in their germline function.

The *C. elegans* genome encodes a paralog of PLP-1, named as PLP-2; these proteins share a high degree of amino acid sequence similarity (Fig. S1). To test whether PLP-2 could functionally substitute PLP-1, we generated *plp-1(ok2155); plp-2(ok2153)*. *ok2153* deletes the entire coding sequence of *plp-2*. Similar to *plp-1* and *plp-2* single mutants that were all fertile (n = 200), all the *plp-1; plp-2* double mutants were also fertile (n = 200). Moreover, in contrast to the sterility observed in *puf-8; plp-1* worms, none of the *puf-8; plp-2* worms were sterile (n = 200). These results indicate that *plp-2* does not functionally overlap with *plp-1* in the germ line.

To more precisely determine the *puf-8; plp-1* defect, we examined germ cell nuclei at different stages of development in animals grown at 20°C. For this, we visualized the chromatin

morphology of germ cells, which is unique to each developmental stage, by staining with the DNA-binding dye DAPI. Germ cells in *C. elegans* hermaphrodites develop within two hairpin-shaped tubes, called the gonadal arms. Both gonadal arms are closed at one end, known as the distal end and open at the other end, known as the proximal end. Both gonadal arms open into a common uterus at their proximal ends. The germline stem cells (GSCs) are present at the distalmost part; they progress through the various stages of meiosis and gametogenesis as they migrate proximally. All germ cells present within a gonadal arm are usually referred to as the germ line. As observed in wild-type germ lines, germ cell nuclei of all developmental stages, including the two types of gametes, were present in both *puf-8* and *plp-1* single mutant germ lines. By contrast, at least four kinds of defects could be observed in *puf-8; plp-1* double mutant hermaphrodite germ lines: about 75 % of them did not have any oocytes and had only sperm at the proximal end; 19% had proliferating cells at the proximal end, reminiscent of the germ cell tumors observed in *puf-8* mutant worms raised at 25°C (Subramaniam and Seydoux, 2003); about 4 % had neither type of gametes; and the remaining 2 % had both oocytes and sperm (n = 712) (Fig. 1 and data not shown). In addition, these germ lines were shorter and had fewer germ cells in the distal part when compared to wild type and the two single mutants. However, no obvious defects were observed in *puf-8; plp-1* male germ lines when compared to *puf-8* mutants (Fig. S2).

In *C. elegans* hermaphrodites, absence of oocytes can result from defects in either spermatogenesis-to-oogenesis switch or oocyte development. To distinguish between these two possibilities, we feminized the germ lines using a *fem-3* loss-of-function mutation [*fem-3(e1996)*], which eliminates spermatogenesis without affecting oogenesis (Ahringer and Kimble, 1991; Barton et al., 1987; Hodgkin, 1986). As expected, *fem-3*, *puf-8; fem-3* and *plp-1 fem-3* germ lines produced only oocytes, whereas no gametes were seen in *puf-8; plp-1 fem-3* triple mutant germ lines (Fig. S3). Similarly, 95 % of *puf-8; plp-1* germ lines (n = 260) did not produce any gametes when depleted of FOG-2, another protein required for spermatogenesis (Schedl and Kimble, 1988). These observations point to a role for both *puf-8* and *plp-1* in oocyte development, and show that at least one of these two genes must be active for normal oogenesis.

Simultaneous loss of PUF-8 and PLP-1 had only a marginal effect on germ cell proliferation. The number of metaphase nuclei, detected by immunostaining with anti-phosphohistone H3 antibodies, was slightly reduced in the mitotic zone of *puf-8; plp-1* germ lines (Fig. S4).

However, the excessive proliferation of germ cells caused by gain-of-function mutations in *glp-1*, a gene required for GSC maintenance (Pepper et al., 2003), was unaffected by the loss of *puf-8* and *plp-1*. Excessive proliferation has also been observed in *gld-2; gld-1* double mutants; these two genes function in a redundant fashion to promote meiotic entry (Kadyk and Kimble, 1998). Even here, loss of PUF-8 and PLP-1 had no effect: we did not see any reduction in the size of proliferating germ cell population in *gld-2; gld-1; puf-8; plp-1* quadruple mutants when compared to *gld-2; gld-1* double mutants (Fig. S5). Both PUF-8 and PLP-1 could be dispensed for the meiotic entry as well: the expression pattern of HIM-3, a synaptonemal complex protein that is often used as a meiotic marker (Zetka et al., 1999), was not altered in *puf-8; plp-1* germ lines (Fig. S4).

The *plp-1* single mutant worms display temperature-sensitive sterility phenotype

We wished to test whether *plp-1* single mutants, like *puf-8* single mutants, display any temperature-sensitive phenotype. For this, we shifted embryos collected from wild-type and *plp-1(ok2155)* hermaphrodites maintained at 20°C to 25°C and allowed them to hatch and develop to adulthood at 25°C. Embryos of both genotypes hatched and reached the adult stage normally. However, while all wild-type embryos developed into fertile adults (n = 114), none of *plp-1* adults were fertile (n = 248; Table S2). A similar observation has been made by another independent study published while this work was progressing (Lalani et al., 2014). A closer look at germ cells by DAPI-staining revealed that the majority of *plp-1* germ lines did not produce oocytes, whereas a few of them developed germ cell tumors at the proximal end at about 72 hours after hatching. Even these few did not have any oocytes (Fig. 2). However, a few oocytes could be seen in 63 % of *plp-1* germ lines a day later (2-day-old adults; n = 162). These oocytes were presumably defective, as a few of them appeared to have undergone endomitotic reduplication. None of *plp-1* worms grown at 25°C produced embryos even after 120 hours after hatching (n = 68). These results reveal an essential function for *plp-1* in oocyte development at elevated temperatures.

PLP-1 is essential in males for mating

Our attempts to generate *plp-1(ok2155)* males uncovered a role for PLP-1 in the mating process. We obtained *plp-1(ok2155/+)* heterozygous males by mating *plp-1(ok2155/ok2155)* hermaphrodites with wild-type males, and backcrossed them with *plp-1(ok2155/ok2155)* hermaphrodites. The resulting male progeny were backcrossed again and this process was repeated for several successive generations. Genotyping of the male progeny by PCR revealed the presence of *plp-1(ok2155/ok2155)* homozygous males among the progeny. However, approximately 50 % of male progeny were heterozygous even after 10 successive backcrosses. We then tested the ability of these males to mate by setting up 24 single-male crosses with *fem-3(e1996)* hermaphrodites, which, as mentioned above, do not produce any sperm but produce normal oocytes. We genotyped the male parents of these crosses after allowing sufficient time for mating (48 hours). While 12 out of 16 *plp-1(ok2155/+)* heterozygous males sired progeny, none of the 8 *plp-1(ok2155/ok2155)* homozygous males sired progeny (Table S3). The *fem-3(e1996)* hermaphrodites used in these crosses did produce progeny when subsequently mated with wild-type males, indicating that these hermaphrodites were not defective in producing oocytes or mating. We inspected the germ lines of males that failed to sire progeny by staining with DAPI and found that the sperm production in these males was normal. However, the *plp-1* males did not show normal mating behavior: unlike wild-type males, *plp-1* males did not stop forward locomotion upon encountering a hermaphrodite, or go around the hermaphrodite in search of vulva. Consistently, we did not find any sperm in the uterus of hermaphrodites mated with these males (data not shown). Thus, the failure of *plp-1* males to sire progeny most likely resulted from some somatic defect that compromised their normal mating behavior.

PLP-1 localizes to P granules throughout the germ line and to similar perinuclear granules in some somatic cells

To begin to understand how PLP-1 functions in the germ line, we determined its expression pattern using both PLP-1-specific antibodies and an integrated transgene that expresses PLP-1::GFP under the control of *plp-1* promoter and 3′ UTR. This transgene restored fertility in *puf-8; plp-1* mutants, indicating that the GFP fusion did not interfere with PLP-1 activity (data not shown). As shown in Fig. 3A, PLP-1 was present throughout the germ line, with prominent concentration on granules arranged in what appeared as perinuclear circles. Distribution of PLP-1 in the core cytoplasm was more readily noticeable in unfixed, live germ lines expressing the *plp-1::gfp* transgene. Similar distribution patterns were observed in both hermaphrodite and male germ lines. In worms expressing the *plp-1::gfp* transgene, we noticed GFP fluorescence in several cells surrounding the pharyngeal bulbs (Fig. 3B) and in cells in the tail region (Fig. 3C). Even in these somatic cells, PLP-1::GFP was concentrated on perinuclear granules, in addition to being present in the cytoplasm. Both *plp-1::gfp* transgene and anti-PLP-1 antibodies revealed the presence of PLP-1 in the cytoplasm of both somatic and germline blastomeres throughout embryonic development (Figs 3D, 4B, S6). Similar localization patterns were observed using the mCherry tag as well, and in worms in which the endogenous PLP-1 was tagged with GFP (data not shown).

We confirmed that the PLP-1 circles were indeed perinuclear by using the nuclear membrane marker, EMR-1::mCherry (Fig. 4A) (Pushpa et al., 2013). To determine whether PLP-1 is a component of P granules, we generated double transgenic lines expressing both PLP-1::GFP and a RFP-tagged version of PGL-1, which is a core component of P granules (Kawasaki et al., 1998; Wolke et al., 2007). We found that PLP-1::GFP indeed colocalized with PGL-1::RFP in both adults and embryos (Fig. 4B). Intriguingly, unlike in adult germ lines, not all PLP-1::GFP granules colocalized with PGL-1::RFP in embryos. Localization of PLP-1 on perinuclear granules in the germ line could be detected in anti-PLP-1-immunostained embryos as well (Fig. S6).

Localization of PLP-1 to P granules in embryos has been observed earlier as well (Witze et al., 2009). However, in contrast to the previous study, which found PLP-1 mostly in the nuclei of embryos (Witze et al., 2009), we did not observe any detectable nuclear localization of PLP-1 in the transgenic reporter lines described above or in germ lines and embryos immunostained with PLP-1-specific antibodies. We think differences in antibody specificities and immunostaining conditions are the probable causes of the variation between the earlier and our observations.

PLP-1 is essential for silencing transgenes and piRNA targets in the germ line, and for robust RNAi response

PUF-8 regulates the translation of several mRNAs in the germ line by acting via their 3′ UTR sequences (Maheshwari et al., 2016; Mainpal et al., 2011; Vaid et al., 2013). Transgenic reporter strains suitable for assaying 3′ UTR activity in the germ line are available in our laboratory for several potential targets of PUF-8. The redundancy between *puf-8* and *plp-1* described above prompted us to screen these reporter strains to test whether PLP-1 affected the reporter expression in any of them. In the case of *gfp*::*H2B*::*pal-1* 3′ UTR transgene, GFP::H2B expression was seen in oocytes, which is similar to the endogenous PAL-1 expression pattern, but only in worms grown at 25°C (Mainpal et al., 2011). By contrast, when this transgene was introduced into *plp-1* worms, GFP::H2B could be readily detected in oocytes even when the worms were grown at 20°C (Fig. 5). Except this, we did not see any other alterations in the expression pattern. We reasoned that the *pal-1* 3′ UTR transgene might be silenced in the germ line at 20°C, and this silencing might be dependent on PLP-1. To test this, we introduced two other integrated transgenes, namely *gfp::gld-1* and *gfp::pgl-1*, into the *plp-1(ok2155)* genetic background. These two transgenes have been previously shown to be silenced in the germline at 20°C (Cheeks et al., 2004; Merritt et al., 2008). Consistent with our reasoning, both these transgenes remained active in *plp-1* germ lines for at least 100 generations at 20°C (we did not observe beyond this), whereas they became silent within three generations in wild-type germ lines (Fig. 5).

Extrachromosomal DNA arrays, consisting of multiple tandem repeats, are readily silenced in wild-type germ lines at 20°C. To test whether PLP-1 is involved in this process as well, we checked the effect of *plp-1* mutation on the expression of *ccEx7271*extrachromosomal array, which expresses GFP under the control of *let-858* promoter and has been shown to be silenced in the germ line (Kelly et al., 1997; Tabara et al., 1999b). As expected, *ccEx7271* array became silent in the first generation itself at 20°C in control germ lines. By contrast, it remained active for at least 30 generations in the *plp-1(ok2155)* genetic background (Fig. 5).

Next, we compared the expression of two different piRNA sensors in wild-type and *plp-1* germ lines. Both these piRNA sensors have been shown to faithfully reflect the status of piRNA-mediated gene silencing in the germ line (Bagijn et al., 2012). As shown in Fig. 5, both the piRNA sensors were silenced in wild-type germ lines by the third generation, but remained active in *plp-1* germ lines even at the 90th generation, demonstrating that PLP-1 is essential for the piRNA-mediated silencing as well.

Mutants defective for silencing foreign genetic elements in the germ line have been shown to be resistant to RNAi (Tabara et al., 1999b). Therefore, we targeted three different genes, namely *mex-3*, *pos-1* and *spn-4*, by RNAi and compared the levels of RNAi penetrance between wild-type and *plp-1* worms. These three genes were chosen because depletion of proteins encoded by them results in fully-penetrant embryonic lethality (Huang et al., 2002; Tabara et al., 1999a). The penetrance of *mex-3(RNAi)* did not vary significantly between wild-type and *plp-1* worms (Table S4). However, about 12 % of *pos-1(RNAi)* and about 15 % of *spn-4(RNAi)* embryos of *plp-1* worms were viable (n = 1368 and 1590, respectively), whereas only about 1.2 % of *pos-1(RNAi)* and about 1.4 % of *spn-4(RNAi)* embryos of wild-type worms were viable (n = 1901 and 1805, respectively), revealing a slight reduction in the ability of *plp-1* worms to elicit RNAi response. Thus, although the RNAi-mediated gene silencing per se does not depend on *plp-1*, its robustness does appear to require *plp-1*.

PLP-1 participates in the initiation of germline gene silencing

Some factors, such as PRG-1, initiate transgene silencing in the germ line, while others, such as MUT-2/RDE-3 and MUT-7, maintain the silenced state (Lee et al., 2012; Shirayama et al., 2012). This functional distinction among the components of silencing pathways prompted us to determine whether PLP-1 functions during the initiation and/or maintenance of silencing for the *gfp::pgl-1* transgene, *ccEx7271* extrachromosomal array and piRNA sensor-1 that we tested in experiments described in the preceding section. When introduced from strains in which these were already silenced, all three sequences remained silent in the *plp-1*mutant background even after 10 generations. By contrast, they became active at the first generation itself when introduced into the *rde-3* mutant background (Fig. 6). Taken together, these observations and results presented in the preceding section indicate that PLP-1 functions only during the initiation step of transgene silencing, and is dispensable for the maintenance step for the three sequences tested here.

PLP-1 is not essential for small RNA biogenesis

Germline gene silencing depends on the generation of small RNAs. In some silencing-defective mutants, the biogenesis of small RNAs is disrupted. For instance, piRNAs are not produced in *prg-1* mutants (Batista et al., 2008). Therefore, we profiled small RNA transcripts using high throughput sequencing and compared the levels of different classes of small RNAs among wild-type (positive control), *prg-1* (negative control) and *plp-1* worms. Although there were slight changes in relative contributions of the different classes, the levels of transcripts of all classes were comparable between wild-type and *plp-1* worms. By contrast, consistent with the previous findings, piRNAs were absent in *prg-1* mutants assayed in parallel (Fig. 7, Supplementary dataset-1). Based on a cutoff of 4-fold, 312 mRNAs had differential levels of small RNAs in *plp-1* relative to wild type. However, they were not enriched for any specific class of small RNAs. Furthermore, despite the involvement *plp-1* in the silencing of piRNA sensors (Fig. 5), levels of piRNAs are not reduced in *plp-1* mutants. These results indicate that *plp-1* is not

essential for the biogenesis of small RNAs, and suggest that it may function at a step downstream of small RNA synthesis in the silencing pathways.

Loss of PLP-1 affects the expression of the same set of endogenous germline genes as germline gene-silencing pathways

Disruption of germline gene-silencing pathways leads to an increase in the expression levels of several endogenous genes. For example, the levels of more than two thousand endogenous mRNAs are significantly higher in *prg-1* mutants when compared to wild type (Bagijn et al., 2012; Lee et al., 2012; Reed et al., 2020). Similarly, the transcription of about 1600 genes has been shown to be upregulated in *mut-16* mutants (Phillips et al., 2012; Reed et al., 2020). This prompted us to investigate whether the expression patterns of endogenous genes are similarly altered in *plp-1* mutants. We generated transcriptome profiles for both wild-type and *plp-1* mutant genotypes using high throughput sequencing and compared the two. Such a comparison identified 1367 genes as differentially expressed between wild-type and *plp-1* animals with a cutoff value of ≥ 2-fold difference; of these, 780 were upregulated and 587 were downregulated in *plp-1* (Supplementary dataset-2). RNA from 20°C-grown hermaphrodites were used for transcriptome profiling, and as shown in Fig. 1, the germline architecture of *plp-1* mutants grown at 20°C did not display any noticeable defects, and was comparable to wild type. Thus, the observed differential expression unlikely resulted from changes in the number or kind of cells in the germ line.

While genes belonging to diverse classes—classified based on potential or confirmed biochemical functions—were represented in both upregulated and downregulated groups, three classes stood out: there were 57 sperm-related genes, 53 collagen and other cuticle-related genes, and 52 genes encoding protein kinases among the genes upregulated in *plp-1* mutants (Fig. 8A). By contrast, there were only one sperm-related and nine cuticle-related genes in the downregulated group. On the other hand, genes encoding transcription factors and nuclear hormone receptors (30), heme-binding and oxidoreductases (20) and histones (9) were more represented in the downregulated group. We performed quantitative reverse transcription-polymerase chain reaction (qRT-PCR) for 18 sperm-related genes in the upregulated group, and

found that the transcript levels of all 18 were indeed higher in *plp-1* mutants when compared to wild type (Fig. 8B). Furthermore, we compared the transcript abundance between soma and germ line for 5 of the above 18. All five were germline-enriched, and their upregulation in *plp-1* mutants primarily resulted from an increase in the germ line, rather than soma (Fig. S7).

Many endogenous genes upregulated in *prg-1* mutants were also found to be upregulated in *mut-16* mutants (Reed et al., 2020). These common gene expression changes probably resulted from the disruption of gene-silencing pathways in these two mutants. Since *plp-1* mutants as well displayed gene-silencing defects, we expected a significant overlap among the sets of genes upregulated in *prg-1*, *mut-16* and *plp-1* mutants. This indeed was the case: 44 % of the 780 genes upregulated in *plp-1* were also in the class shown to be upregulated in *mut-16* ($p < 9.6 \times 10^{-176}$), and this number increased to 57 % when *plp-1* and *prg-1* sets were compared ($p < 8.8 \times 10^{-203}$). We found 316 genes—a little over 40 % of the 780 genes—to be common to all three sets (Fig. 9).

About 34 % of genes upregulated in *prg-1* and 36 % of genes upregulated in m*ut-16* mutants belong to the "germline-enriched" category as defined by (Reed et al., 2020; Reinke et al., 2004). We noticed a similar trend with *plp-1* as well: 36 % of genes upregulated in *plp-1* mutants belong to this category. Strikingly, when only the germline-enriched subsets were compared, 95 % of genes upregulated in *plp-1* mutants have been found to be upregulated in *prg-1* mutants as well ($p < 0.000e+00$); this overlap is 77 % between *plp-1* and *mut-16* mutants ($p < 3.6 \times 10^{-281}$). Overall, 211 germline-enriched genes were found to be upregulated in all three mutants, and 96 % of these (202 / 211) are spermatogenesis-related, indicating that the same components that silence transgenes and other foreign genetic elements in the germ line might also control the expression of spermatogenesis-related genes (Fig. 9). In mutants such as *mut-16* and *set-2*, and in germ lines depleted of P granules, some soma-enriched genes are misexpressed in the germ line (Knutson et al., 2017; Robert et al., 2014; Rogers and Phillips, 2020). We did not find significant overlap between these soma-enriched gene sets and the set of genes upregulated in *plp-1* mutants (Supplementary dataset-2). Furthermore, only 22 of the 780 genes upregulated in *plp-1* belong to the soma-enriched category. Conversely, the 306 genes upregulated in *plp-1*, but not in *prg-1* or *mut-16*, were more or less excluded from the germline-enriched class (Fig. 9). We randomly chose 5 of the 306 genes and validated their differential expression by qRT-PCR, and found two of them to be upregulated in *plp-1* mutant germ lines (Fig. S8). Thus, in the germ

line, *plp-1* may not play a major role in suppressing somatic genes, although it may suppress a few non-germline-enriched genes.

As mentioned in the Introduction, some small RNAs called WAGO-22G-RNAs associate with WAGOs, while others with CSR-1 in *C. elegans*. In *prg-1* mutants, mRNAs targeted by WAGO-22G-RNAs, but not the CSR-1-22G RNAs, have been found to be upregulated (Lee et al., 2012). We examined the set of genes differentially expressed in *plp-1* mutants and found that the targets of WAGO-22G-RNAs were more or less equally represented in both upregulated and downregulated groups, although neither group was enriched for these targets. By contrast, CSR-1-22G-RNA targets were almost completely excluded from both groups (Fig. 9). Thus, *plp-1* does not appear to be engaged directly in the CSR-1 pathways.

DISCUSSION

We have identified PLP-1 as a component of the germline gene-silencing pathway. We have shown that PLP-1 functions in silencing extrachromosomal arrays, integrated transgenes, and piRNA sensors. Like many AGOs, PLP-1 localizes to P granules, and loss of PLP-1 cause temperature-sensitive germline defects, much like some of the other silencing pathway mutations. Furthermore, our work reveals a remarkable overlap among the sets of germline-related genes upregulated in *plp-1* mutants and two other mutants, namely *prg-1* and *mut-16* mutants, which are known to disrupt gene-silencing pathways.

We identified *plp-1* based on its genetic interaction with *puf-8*: both *puf-8* and *plp-1* single mutants are fertile at 20°C, but the *puf-8; plp-1* double mutants are sterile at this temperature. The encoded proteins of these two genes do not share sequence or structural similarity. PUF-8 is a PUF family protein containing the conserved PUF RNA-binding domain (Wickens et al., 2002). Like many other PUF proteins, PUF-8 regulates translation by binding to specific 3′ UTR sequences of its target mRNAs (Maheshwari et al., 2016; Mainpal et al., 2011; Vaid et al., 2013). On the other hand, PLP-1 shares sequence similarity with Pur repeat-containing proteins such as the human Pur-alpha (Fig. S9) (Daniel and Johnson, 2018). The Pur proteins bind both single-stranded DNA and RNA through their Pur repeats, which are well conserved from bacteria to human (Bergemann et al., 1992; Chepenik et al., 1998). The Pur repeat—named after the human

ortholog which binds purine-rich single-stranded DNA—shares neither sequence nor structural similarity with the PUF domain. Although Pur-alpha has been implicated in translational regulation (Gallia et al., 2001), it does not seem to regulate translation the way PUF proteins do, i.e., by binding to the 3′ UTR of specific target mRNAs. Consistent with this notion, none of the 3′ UTR reporter fusions regulated by PUF-8 showed any change in expression when introduced into *plp-1* mutants (unpublished observations by L. T., R. V. and K.S.). Therefore, we do not think PUF-8 and PLP-1 substitute each other biochemically. However, there are some notable similarities: both proteins potentially bind RNA and protein, and localize to P granules (Ariz et al., 2009; this study). Both *puf-8* and *plp-1* single mutants display temperature-sensitive sterility phenotype (Subramaniam and Seydoux, 2003; this study). In addition, PUF-8 and the mammalian ortholog of PLP-1 are implicated in mRNA transport (Johnson et al., 2006; Kanai et al., 2004; Pushpa et al., 2013). Thus, PUF-8 and PLP-1 may control gene expression at the RNA level, but through different biochemical mechanisms. For example, PLP-1 may control the levels of certain germline mRNAs, while PUF-8 may regulate their translation. In such a scenario, it is not difficult to imagine how increased mRNA levels, when combined with a lack of translational control could have damaging consequences, while either one alone might be inconsequential. Alternatively, PUF-8 and PLP-1 may contribute to P granule integrity such that their simultaneous absence, but not the absence of either one, perturbs the integrity of P granules sufficiently enough to alter the stability and/or translation of mRNAs associated with these granules. Such a perturbation may also happen under temperature stress (25°C) in the absence of either of these two proteins, given the liquid-droplet like nature of P granules. A third possibility is that PUF-8 facilitates the P granule association of PLP-1, or vice versa, but we did not see any alteration in the localization of either protein in the absence of the other (unpublished observations by L. T., R. V. and K.S.).

Germline gene-silencing pathway components such as PRG-1 and *mutator* proteins are involved in the formation of small RNAs. While PRG-1 is essential for the accumulation of piRNAs, *mutator* proteins such as MUT-16 contribute to silencing through their facilitation of siRNA amplification (Batista et al., 2008; Phillips et al., 2012). By contrast, our results reveal that PLP-1 is not essential for small RNA accumulation (Fig. 7). Thus, PLP-1 must function downstream of small RNA biogenesis in the silencing pathways. How does PLP-1 contribute to gene silencing in the germ line? Although PLP-1 is not essential for survival of *C. elegans*, its

mouse ortholog is essential for survival (Khalili et al., 2003). The Pur proteins participate in a variety of cellular functions such as transcription, translation, activation of Cdk9 and mRNA transport (Darbinian et al., 2001; Gallia et al., 2001; Johnson et al., 2006; Kanai et al., 2004; Zhang et al., 2005). It has been proposed that the remarkable versatility of Pur proteins emerges from their ability to interact with both single-stranded nucleic acids and other proteins. During the course of evolution, the Pur proteins seem to have retained their ability to bind single-stranded nucleic acids by conserving the amino acid sequence of Pur repeats, which interact with nucleic acids. At the same time, these proteins seem to have adapted themselves to diverging cellular needs by interacting with new protein partners, probably facilitated by the diversification of the C-terminal region involved in protein-protein interactions (Daniel and Johnson, 2018). We think this flexibility most likely enables PLP-1 to couple, or strengthen the interaction among, some of the proteins and RNAs in the germline gene-silencing machinery. The notion that PLP-1 may facilitate RNA-protein interactions in P granule-like structures might explain its role in the somatic cells as well, where again we find PLP-1 on granules. Identifying the protein partners of PLP-1 will help test this idea and provide mechanistic insights into its function.

An earlier study implicated PLP-1 in the transcriptional modulation of the endoderm-specific transcription factor END-1 (Witze et al., 2009). It is conceivable that PLP-1 regulates transcription, at least of some genes, in the germ line as well. Misexpression of these genes in the absence of PLP-1 can potentially interfere with the germline gene-silencing machinery, and thus account for the silencing defects of *plp-1* mutants. One paradox that remains in need of explanation is why PLP-1 localizes primarily on cytoplasmic granules in the germ line and soma. Although we cannot formally rule out the presence of PLP-1 in nuclei, results from three independent types of experiments, described in the Results section, demonstrate the cytoplasmic, perinuclear granules to be the major sites of PLP-1 localization in both the tissues. This localization pattern of PLP-1 and its involvement in germline gene-silencing are strikingly similar to that of many other silencing pathway components. Therefore, we favor a model in which the predominant function of PLP-1 is in P granules and similar RNA granules in the soma, where it facilitates RNA-protein interactions. This model may be useful to explain the functions of Pur proteins found on RNA granules in other organisms such as *Drosophila* and mammals (Aumiller et al., 2012; Kanai et al., 2004).

MATERIALS AND METHODS

Strain maintenance and genetic crosses

All *C. elegans* strains used in this study were maintained as per established protocols at 20°C, unless mentioned otherwise (Brenner, 1974). Strains of different genotypes used in this study were constructed using standard genetic crosses. Briefly, strains carrying the integrated transgenes, GFP::H2B::pal-1 3′ UTR, GFP::PGL-1 and GFP::GLD-1, and the ccEx7271 extrachromosomal array were maintained in active state at 25°C. They were mated with *plp-1(+/-)* males at 25°C; the progeny were shifted to 20°C and cloned. The transgenes and the *ok2155* allele of *plp-1* were detected by single-worm PCRs and animals homozygous for both the transgene and *ok2155* were obtained by further cloning and single-worm PCRs (Fig. S10). Similar strategy was employed for the piRNA sensor 21UR-1349 as well. The piRNA sensor 21UR-1 was transferred from the *prg-1(-)* background [strain SX1288], in which it is active, into the *plp-1* mutant. Maintenance at 20°C of strains carrying the transgenes, extrachromosomal array and piRNA sensors mentioned above for several generations led to complete silencing. Such silenced transgenes—their presence was detected by PCR—were then introduced into *plp-1* and *rde-3* mutants through crosses setup at 20°C. All strains used in this study are listed in Table S5.

RNA interference

Coding sequences of target genes were PCR-amplified from cDNA and inserted at the EcoRV site of pSV2 vector by the TA cloning method. Sequences of PCR primers are listed in Table S2. Both strands of inserts cloned into pSV2 vector are transcribed into dsRNA when introduced into the HT115 bacterial strain (Mainpal et al., 2011). RNAi was performed by the feeding method described by Timmons et al (Timmons et al., 2001). For depleting PLP-1 by RNAi, L4 larvae were transferred to RNAi lawns and transferred to fresh RNAi lawns 24 hours later. Embryos collected for 8-12 hours on the fresh lawns were allowed to hatch and grow to adulthood. Phenotypes of these adults were scored. In the case of *mex-3*, *pos-1* and *spn-4*, gravid hermaphrodites were placed on RNAi lawns for 8-12 hours and transferred to fresh RNAi lawns. The worms were removed after they laid embryos for about 8 hours, and the embryos

were counted. Embryos remaining after 24 hours were counted again to determine the fraction of viable progeny.

Generation of anti-PLP-1 antibody

Polyclonal antibodies were raised in rabbits against bacterially-expressed fusion protein containing maltose-binding protein (MBP) and full-length PLP-1 protein (MBP::PLP-1). Coding sequences of PLP-1 were PCR-amplified from cDNA and inserted at the BamH1 site of pMAL-cE plasmid vector which expresses the inserted ORF as an MBP fusion (New England Biolabs). The resulting plasmid was introduced into the *E. coli* strain BL21(DE3). Expression and purification of MBP::PLP-1 were carried out as per standard protocols using IPTG for inducing the expression of fusion protein, and deoxycholic acid for bacterial cell lysis (Sambrook et al., 1989). The MBP::PLP-1 fusion protein, which was mostly in the supernatant following centrifugation of the lysate, was purified by affinity chromatography using HIS-select Cartridge following manufacturer's protocols (Sigma-Aldrich Cat. No. H8286).

Rabbit antiserum against MBP::PLP-1 was produced at a commercial facility (Bangalore Genei) and antibodies specific for PLP-1 were purified from the antiserum using bacterially-produced GST::PLP-1 as the affinity tag. For this, the bacterial cell lysate containing GST-PLP-1 was separated on SDS-PAGE and transferred to nitrocellulose membrane. Protein bands were visualized by staining with Amido black, and the strip of membrane containing GST::PLP-1 was cut and incubated with the anti-MBP::PLP-1 antiserum, after washing-off the dye. The bound anti-PLP-1 antibodies were eluted in 0.2M glycine, 1mM EGTA at pH 2.8. The pH of the eluate was adjusted to 7.0 by adding 0.1 volume of 1M Tris base and stored at 4°C.

Generation of transgenic lines

Transgenic lines expressing PLP-1::GFP and mCherry::PLP-1 were generated by biolistic bombardment as described earlier (Jadhav et al., 2008; Praitis et al., 2001). The plasmid construct pLT2, used for introducing the *plp-1:gfp* transgene, carried 2-kb genomic region immediately upstream of the *plp-1* ORF, the *plp-1* ORF (1 kb), the GFP coding sequences and 2-kb genomic region downstream of the *plp-1* stop codon in the pBluescript backbone. In addition, this vector carried a 5.6 kb genomic fragment that rescues the *unc-119(ed3)* defect. The construct pLT5 used for introducing the *mCherry:plp-1* transgene contained the *pie-1* promoter

and *hip-1* 3′ UTR sequences. In this construct, the coding sequences of mCherry were introduced at the N-terminus of PLP-1. At least three independent lines with similar expression patterns were obtained for both transgenes.

To produce PLP-1::GFP from the endogenous locus of *plp-1*, we inserted the coding sequences of GFP in-frame just before the *plp-1* stop codon using the CRISPR/Cas9 method (Arribere et al., 2014). The sgRNA-expressing plasmids and the repair template carrying GFP coding sequences were prepared as described earlier (Kumar and Subramaniam, 2018). Oligonucleotides used in both bombardment and CRISPR/Cas9 experiments are listed in Table S6.

Fluorescence microscopy

For visualization of chromatin in whole worms, worms were collected in PBST (PBS + 0.1% Tween 20) and fixed in precooled methanol (-20°C) for at least 20 minutes. Fixed animals were incubated in methanol containing 25ng/µl DAPI for 20 minutes in dark at room temperature. Stained animals were then washed thrice in PBST and mounted in Vectashield antifading agent (Vector laboratories). For the extrusion of adult germ lines, worms were anesthetized in 2mM levamisole and cut just posterior to pharynx using a 25G injection needle on a microscope slide. Within 10 minutes of dissection, extruded germ lines were fixed in formaldehyde fixative (4% formaldehyde in PBS) for 1 hour at room temperature. Germ lines were then washed thrice with PBST and incubated with PBS containing 25ng/µl DAPI for 30 minutes.

For staining with affinity-purified anti-PLP-1 and anti-PH3 antibodies (Sigma-Aldrich), germ lines dissected and fixed as above were washed twice with blocking buffer (PBS containing 0.1% bovine serum albumin and 0.1% Triton X-100) and incubated in the blocking buffer for 1 hour at room temperature. Antibodies were diluted 1:1000 with blocking buffer and added to germ lines, and were incubated overnight at 4°C. Germ lines were then washed with blocking buffer and incubated with 1:50 diluted anti-rabbit secondary antibodies conjugated with FITC or rhodamine (Jackson ImmunoResearch) for 7-8 hours at 4°C. After washing thrice with blocking buffer, germ lines were mounted in Vectashield. Anti-PLP-1 antibody did not stain any noticeable structures in *plp-1(ok2155)* germ lines or embryos, confirming that the antibody is specific for PLP-1. For immunostaining embryos, embryos were freeze-cracked using liquid

nitrogen and fixed in pre-chilled (-20°C) methanol for 5 minutes at -20°C, followed by 4% formaldehyde for 20 minutes at room temperature. After blocking, the embryos were stained overnight with 1:10-diluted affinity-purified anti-PLP-1 antibodies in a humidity chamber. They were then washed thrice in blocking buffer, and stained with 1:500-diluted anti-rabbit secondary antibodies conjugated with Alexa Fluor 488 (Jackson ImmunoResearch) for 6 hours at room temperature.

Fluorescence signals from whole worms and germ lines prepared as above were observed using Zeiss Axio Imager M2 fluorescence microscope and imaged using Zeiss Axiocam 506 Mono CCD camera. Where necessary, images were deconvolved using the Deconvolution module of Zeiss Axiovision software.

Small RNA sequencing and data analysis

We picked 20-25 young adult stage worms from non-starved plates grown at 20°C into TRIzol reagent (ThermoFisher Scientific, Waltham, MA). RNA was purified from TRIzol following standard guidelines from (Johnstone, 1999). Small RNAs were then purified with a mirVana kit through a modified protocol optimized for small sample input (Ambion, ThermoFisher Scientific, Waltham, MA). Briefly, total RNA was mixed with MirVana lysis/binding buffer and homogenate buffer and incubated at room temperature for 5 minutes, and then small RNAs were purified through two rounds of alcohol precipitation. In the first we added one third the volume of ethanol, centrifuged at 5000 rpm for 5 minutes, and then transferred the supernatant to a fresh tube. In the second round of extraction, we added one volume of isopropanol and centrifuged at 15000 rpm for 30 minutes. The purified small RNAs were treated with Cap-Clip enzyme to convert all 5’ ends to monophosphate, after which libraries were made with a TruSeq small RNA kit and sequenced on a miSeq instrument (Illumina, San Diego, CA).

For data analysis, reads were trimmed for adapter sequence at the 3' end and aligned to the C. *elegans* protein coding (WS245) and ncRNA transcriptomes. Counts of reads to each gene were generated using custom Python scripts.

Transcriptome sequencing

Total RNA was isolated from adult hermaphrodites using TRI reagent (Sigma-Aldrich) as per manufacturer's protocols. Three biological replicates were used for transcriptome sequencing at a commercial facility (Macrogen). After removing potential DNA contamination by DNase treatment, polyA+ RNA was isolated using the TruSeq Stranded mRNA preparation kit (Illumina), which was then fragmented randomly and reverse-transcribed into cDNA. Following adaptor ligation to both ends, the cDNA were PCR-amplified and size-selected for fragments of 200-400-bp length. Both ends of these fragments were sequenced using NovaSeq 6000 S4 Reagent kit in a NovaSeq 6000 NGS sequencing machine (Illumina) following manufacturer's protocols. After removing low quality reads (Phred score <20), adapter sequences were trimmed using the Trimmomatic 0.38 program. Reads shorter than 36 bp were dropped from the trimmed reads data. Trimmed reads were mapped to *C. elegans* reference genome data version WS264 using HISAT2 version 2.1.0 and Bowtie2 2.3.4.1. Reads were aligned into potential transcripts using StringTie version 1.3.4d. Transcripts corresponding to 15,316 genes were selected, after omitting the transcripts with read count 0 in more than 2 of the 6 samples [3 biological replicates each of wild type and *plp-1(ok2155)*], for the differential gene expression analysis, which was performed using the DESeq2 package. Genes fulfilling the condition |fc|>=2 & nbinomWaldTest raw *p*-value<0.05 were selected as differentially expressed, and were annotated using the DAVID tool. Gene enrichment analyses were performed using the DAVID tool available at www.ncbi.nlm.nih.gov. Venn diagrams shown in Fig. 9 were generated using tools available at http://bioinformatics.psb.ugent.be/webtools/Venn/ and https://omics.pnl.gov/software/venn-diagram-plotter. Statistical significance of the overlaps was calculated using the tool available at http://nemates.org/MA/progs/overlap_stats.html.

Quantitation of transcripts using real-time RT-PCR

Total RNA was isolated from 100 1-day-old adult animals using TRI reagent (Sigma-Aldrich) and following manufacturer's protocols. The entire amount of RNA was used for cDNA synthesis using oligo dT primer and Revert Aid reverse transcriptase (ThermoFisher) as per manufacturer's protocols. The final cDNA was diluted to 500µl in TE buffer (10mM Tris, pH 8.0 + 1mM EDTA). The qPCR reactions were performed using a QuantStudio 7 flex Real-Time PCR system and the QuantStudio 6 and 7 flex Real-Time PCR system software V1.3 (Applied

Biosystems). The qPCR reactions contained 1xSYBR Green master mix (Bio-Rad), 300nM each of the two primers and 2µl of the diluted cDNA; the PCR settings were: 95°C – 20secs, 40 cycles of 95°C – 2secs, 60°C – 25secs, which was followed by 60°C – 1 min and 95°C – 15secs. Relative quantities were calculated using ΔΔCt method and normalized using *hip-1* and *act-1* as internal controls. Values from three technical replicates each of three biological replicates were used for calculating the average fold change, and the statistical significance was calculated using Student's t-test.

Acknowledgements

We thank Marc Ridyard and Eric Miska for the piRNA sensor strains SX1286, SX1287, SX1288 and SX2110, and Meetu Seth and Craig Mello for the strain WM250. Some of the *C. elegans* strains used in this study were provided by the *Caenorhabditis* Genetics Center, which is funded by National Institutes of Health Office of Research Infrastructure Programs (P40 OD010440).

Competing interests

The authors declare no competing or financial interests.

Author contributions

Conceptualization: L.T., R.V., K.S.; Methodology: L.T., R.V., L.W., A.F., K.S.; Validation: L.T., R.V., L.W., A.F., K.S.; Formal analysis: L.T., R.V., L.W., A.F., K.S.; Investigation: L.T., R.V., L.W., A.F., K.S.; Resources: A.F., K.S.; Writing - original draft: L.T., R.V., K.S.; Writing - review & editing: K.S.; Supervision: K.S.; Project administration: K.S.; Funding acquisition: K.S.

Funding

Research in the K.S. laboratory is supported by grants from the Department of Biotechnology, Ministry of Science and Technology (BT/PR29010/BRB/10/1694/2018) and the Science & Engineering Research Board, Department of Science and Technology, Ministry of Science and Technology (EMR/2016/002272), Government of India.

References

Ahringer, J. and Kimble, J. (1991). Control of the sperm-oocyte switch in Caenorhabditis elegans hermaphrodites by the fem-3 3' untranslated region. *Nature* 349, 346-8.

Ariz, M., Mainpal, R. and Subramaniam, K. (2009). C. elegans RNA-binding proteins PUF-8 and MEX-3 function redundantly to promote germline stem cell mitosis. *Dev. Biol.* 326, 295-304.

Arribere, J. A., Bell, R. T., Fu, B. X., Artiles, K. L., Hartman, P. S. and Fire, A. Z. (2014). Efficient marker-free recovery of custom genetic modifications with CRISPR/Cas9 in Caenorhabditis elegans. *Genetics* 198, 837-46.

Aumiller, V., Graebsch, A., Kremmer, E., Niessing, D. and Forstemann, K. (2012). Drosophila Pur-alpha binds to trinucleotide-repeat containing cellular RNAs and translocates to the early oocyte. *RNA Biol.* 9, 633-43.

Bagijn, M. P., Goldstein, L. D., Sapetschnig, A., Weick, E. M., Bouasker, S., Lehrbach, N. J., Simard, M. J. and Miska, E. A. (2012). Function, targets, and evolution of Caenorhabditis elegans piRNAs. *Science* 337, 574-578.

Barton, M. K., Schedl, T. B. and Kimble, J. (1987). Gain-of-function mutations of fem-3, a sex-determination gene in Caenorhabditis elegans. *Genetics* 115, 107-19.

Batista, P. J., Ruby, J. G., Claycomb, J. M., Chiang, R., Fahlgren, N., Kasschau, K. D., Chaves, D. A., Gu, W., Vasale, J. J., Duan, S. et al. (2008). PRG-1 and 21U-RNAs interact to form the piRNA complex required for fertility in C. elegans. *Mol. Cell* 31, 67-78.

Bergemann, A. D., Ma, Z. W. and Johnson, E. M. (1992). Sequence of cDNA comprising the human pur gene and sequence-specific single-stranded-DNA-binding properties of the encoded protein. *Mol. Cell. Biol.* 12, 5673-82.

Bernstein, E., Caudy, A. A., Hammond, S. M. and Hannon, G. J. (2001). Role for a bidentate ribonuclease in the initiation step of RNA interference. *Nature* 409, 363-6.

Billi, A. C., Fischer, S. E. and Kim, J. K. (2014). Endogenous RNAi pathways in C. elegans. *WormBook*, 1-49.

Brangwynne, C. P., Eckmann, C. R., Courson, D. S., Rybarska, A., Hoege, C., Gharakhani, J., Julicher, F. and Hyman, A. A. (2009). Germline P granules are liquid droplets that localize by controlled dissolution/condensation. *Science* 324, 1729-32.

Brenner, S. (1974). The genetics of Caenorhabditis elegans. *Genetics* 77, 71-94.

Cheeks, R. J., Canman, J. C., Gabriel, W. N., Meyer, N., Strome, S. and Goldstein, B. (2004). C. elegans PAR proteins function by mobilizing and stabilizing asymmetrically localized protein complexes. *Curr. Biol.* 14, 851-62.

Chepenik, L. G., Tretiakova, A. P., Krachmarov, C. P., Johnson, E. M. and Khalili, K. (1998). The single-stranded DNA binding protein, Pur-alpha, binds HIV-1 TAR RNA and activates HIV-1 transcription. *Gene* 210, 37-44.

Claycomb, J. M., Batista, P. J., Pang, K. M., Gu, W., Vasale, J. J., van Wolfswinkel, J. C., Chaves, D. A., Shirayama, M., Mitani, S., Ketting, R. F. et al. (2009). The Argonaute

CSR-1 and its 22G-RNA cofactors are required for holocentric chromosome segregation. *Cell* 139, 123-34.

Conine, C. C., Batista, P. J., Gu, W., Claycomb, J. M., Chaves, D. A., Shirayama, M. and Mello, C. C. (2010). Argonautes ALG-3 and ALG-4 are required for spermatogenesis-specific 26G-RNAs and thermotolerant sperm in Caenorhabditis elegans. *Proc Natl Acad Sci U S A* 107, 3588-93.

Daniel, D. C. and Johnson, E. M. (2018). PURA, the gene encoding Pur-alpha, member of an ancient nucleic acid-binding protein family with mammalian neurological functions. *Gene* 643, 133-143.

Darbinian, N., Sawaya, B. E., Khalili, K., Jaffe, N., Wortman, B., Giordano, A. and Amini, S. (2001). Functional interaction between cyclin T1/cdk9 and Puralpha determines the level of TNFalpha promoter activation by Tat in glial cells. *J Neuroimmunol* 121, 3-11.

Dodson, A. E. and Kennedy, S. (2019). Germ Granules Coordinate RNA-Based Epigenetic Inheritance Pathways. *Dev. Cell* 50, 704-715 e4.

Eddy, E. M. (1975). Germ plasm and the differentiation of the germ cell line. *International review of cytology* 43, 229-80.

Gallia, G. L., Darbinian, N., Jaffe, N. and Khalili, K. (2001). Single-stranded nucleic acid-binding protein, Pur alpha, interacts with RNA homologous to 18S ribosomal RNA and inhibits translation in vitro. *J. Cell. Biochem.* 83, 355-63.

Gent, J. I., Lamm, A. T., Pavelec, D. M., Maniar, J. M., Parameswaran, P., Tao, L., Kennedy, S. and Fire, A. Z. (2010). Distinct phases of siRNA synthesis in an endogenous RNAi pathway in C. elegans soma. *Mol. Cell* 37, 679-89.

Gerson-Gurwitz, A., Wang, S., Sathe, S., Green, R., Yeo, G. W., Oegema, K. and Desai, A. (2016). A Small RNA-Catalytic Argonaute Pathway Tunes Germline Transcript Levels to Ensure Embryonic Divisions. *Cell* 165, 396-409.

Gu, W., Shirayama, M., Conte, D., Jr., Vasale, J., Batista, P. J., Claycomb, J. M., Moresco, J. J., Youngman, E. M., Keys, J., Stoltz, M. J. et al. (2009). Distinct argonaute-mediated 22G-RNA pathways direct genome surveillance in the C. elegans germline. *Mol. Cell* 36, 231-44.

Guang, S., Bochner, A. F., Pavelec, D. M., Burkhart, K. B., Harding, S., Lachowiec, J. and Kennedy, S. (2008). An Argonaute transports siRNAs from the cytoplasm to the nucleus. *Science* 321, 537-41.

Hodgkin, J. (1986). Sex determination in the nematode C. elegans: analysis of tra-3 suppressors and characterization of fem genes. *Genetics* 114, 15-52.

Huang, N. N., Mootz, D. E., Walhout, A. J., Vidal, M. and Hunter, C. P. (2002). MEX-3 interacting proteins link cell polarity to asymmetric gene expression in Caenorhabditis elegans. *Development* 129, 747-59.

Ishidate, T., Ozturk, A. R., Durning, D. J., Sharma, R., Shen, E. Z., Chen, H., Seth, M., Shirayama, M. and Mello, C. C. (2018). ZNFX-1 Functions within Perinuclear Nuage to Balance Epigenetic Signals. *Mol. Cell* 70, 639-649 e6.

Jadhav, S., Rana, M. and Subramaniam, K. (2008). Multiple maternal proteins coordinate to restrict the translation of C. elegans nanos-2 to primordial germ cells. *Development* 135, 1803-12.

Johnson, E. M., Kinoshita, Y., Weinreb, D. B., Wortman, M. J., Simon, R., Khalili, K., Winckler, B. and Gordon, J. (2006). Role of Pur alpha in targeting mRNA to sites of translation in hippocampal neuronal dendrites. *J. Neurosci. Res.* 83, 929-43.

Johnstone, I. J. (1999). Molecular biology. In *C. elegans A Practical Approach*, (ed. I. Hope), pp. 201-225. New York: Oxford University Press.

Kadyk, L. C. and Kimble, J. (1998). Genetic regulation of entry into meiosis in Caenorhabditis elegans. *Development* 125, 1803-13.

Kanai, Y., Dohmae, N. and Hirokawa, N. (2004). Kinesin transports RNA: isolation and characterization of an RNA-transporting granule. *Neuron* 43, 513-25.

Kawasaki, I., Shim, Y. H., Kirchner, J., Kaminker, J., Wood, W. B. and Strome, S. (1998). PGL-1, a predicted RNA-binding component of germ granules, is essential for fertility in C. elegans. *Cell* 94, 635-45.

Kelly, W. G., Xu, S., Montgomery, M. K. and Fire, A. (1997). Distinct requirements for somatic and germline expression of a generally expressed Caernorhabditis elegans gene. *Genetics* 146, 227-38.

Ketting, R. F., Fischer, S. E., Bernstein, E., Sijen, T., Hannon, G. J. and Plasterk, R. H. (2001). Dicer functions in RNA interference and in synthesis of small RNA involved in developmental timing in C. elegans. *Genes Dev.* 15, 2654-9.

Ketting, R. F., Haverkamp, T. H., van Luenen, H. G. and Plasterk, R. H. (1999). Mut-7 of C. elegans, required for transposon silencing and RNA interference, is a homolog of Werner syndrome helicase and RNaseD. *Cell* 99, 133-41.

Khalili, K., Del Valle, L., Muralidharan, V., Gault, W. J., Darbinian, N., Otte, J., Meier, E., Johnson, E. M., Daniel, D. C., Kinoshita, Y. et al. (2003). Puralpha is essential for postnatal brain development and developmentally coupled cellular proliferation as revealed by genetic inactivation in the mouse. *Mol. Cell. Biol.* 23, 6857-75.

Kumar, G. A. and Subramaniam, K. (2018). PUF-8 facilitates homologous chromosome pairing by promoting proteasome activity during meiotic entry in C. elegans. *Development* 145.

Knutson, A. K., Egelhofer, T., Rechtsteiner, A. and Strome, S. (2017). Germ granules prevent accumulation of somatic transcripts in the adult Caenorhabditis elegans germline. *Genetics* 206, 163-178.

Lalani, S. R., Zhang, J., Schaaf, C. P., Brown, C. W., Magoulas, P., Tsai, A. C., El-Gharbawy, A., Wierenga, K. J., Bartholomew, D., Fong, C. T. et al. (2014). Mutations in PURA cause profound neonatal hypotonia, seizures, and encephalopathy in 5q31.3 microdeletion syndrome. *Am. J. Hum. Genet.* 95, 579-83.

Lee, H. C., Gu, W., Shirayama, M., Youngman, E., Conte, D., Jr. and Mello, C. C. (2012). C. elegans piRNAs mediate the genome-wide surveillance of germline transcripts. *Cell* 150, 78-87.

Lev, I., Toker, I. A., Mor, Y., Nitzan, A., Weintraub, G., Antonova, O., Bhonkar, O., Ben Shushan, I., Seroussi, U., Claycomb, J. M. et al. (2019). Germ Granules Govern Small RNA Inheritance. *Curr. Biol.* 29, 2880-2891 e4.

Maheshwari, R., Pushpa, K. and Subramaniam, K. (2016). A role for post-transcriptional control of endoplasmic reticulum dynamics and function in C. elegans germline stem cell maintenance. *Development* 143, 3097-108.

Mainpal, R., Priti, A. and Subramaniam, K. (2011). PUF-8 suppresses the somatic transcription factor PAL-1 expression in C. elegans germline stem cells. *Dev. Biol.* 360, 195-207.

Merritt, C., Rasoloson, D., Ko, D. and Seydoux, G. (2008). 3' UTRs are the primary regulators of gene expression in the C. elegans germline. *Curr. Biol.* 18, 1476-82.

Pak, J. and Fire, A. (2007). Distinct populations of primary and secondary effectors during RNAi in C. elegans. *Science* 315, 241-4.

Parrish, S. and Fire, A. (2001). Distinct roles for RDE-1 and RDE-4 during RNA interference in Caenorhabditis elegans. *RNA* 7, 1397-402.

Pepper, A. S., Killian, D. J. and Hubbard, E. J. (2003). Genetic analysis of Caenorhabditis elegans glp-1 mutants suggests receptor interaction or competition. *Genetics* 163, 115-32.

Phillips, C. M., Montgomery, T. A., Breen, P. C. and Ruvkun, G. (2012). MUT-16 promotes formation of perinuclear mutator foci required for RNA silencing in the C. elegans germline. *Genes Dev* 26, 1433-44.

Praitis, V., Casey, E., Collar, D. and Austin, J. (2001). Creation of low-copy integrated transgenic lines in Caenorhabditis elegans. *Genetics* 157, 1217-26.

Pushpa, K., Kumar, G. A. and Subramaniam, K. (2013). PUF-8 and TCER-1 are essential for normal levels of multiple mRNAs in the C. elegans germline. *Development* 140, 1312-20.

Reed, K. J., Svendsen, J. M., Brown, K. C., Montgomery, B. E., Marks, T. N., Vijayasarathy, T., Parker, D. M., Nishimura, E. O., Updike, D. L. and Montgomery, T. A. (2020). Widespread roles for piRNAs and WAGO-class siRNAs in shaping the germline transcriptome of Caenorhabditis elegans. *Nucleic Acids Res.* 48, 1811-1827.

Reinke, V., Gil, I. S., Ward, S. and Kazmer, K. (2004). Genome-wide germline-enriched and sex-biased expression profiles in Caenorhabditis elegans. *Development* 131, 311-23.

Robert, V. J., Mercier, M. G., Bedet, C., Janczarski, S., Merlet, J., Steve Garvis, S., Ciosk, R. and Francesca Palladino, F. (2014). The SET-2/SET1 histone H3K4 methyltransferase maintains pluripotency in the Caenorhabditis elegans Germline. *Cell Rep.* 9, 443-450.

Rogers, A. K. and Phillips, C. (2020). RNAi pathways repress reprogramming of C. elegans germ cells during heat stress. *Nucleic Acids Res.* 48, 4256-4273.

Sambrook, J., Fritsch, E. F. and Maniatis, T. (1989). Molecular Cloning, a Laboratory Manual. Cold Spring Harbor, New York: Cold Spring Harbor Laboratory Press.

Schedl, T. and Kimble, J. (1988). fog-2, a germ-line-specific sex determination gene required for hermaphrodite spermatogenesis in Caenorhabditis elegans. *Genetics* 119, 43-61.

Sheth, U., Pitt, J., Dennis, S. and Priess, J. R. (2010). Perinuclear P granules are the principal sites of mRNA export in adult C. elegans germ cells. *Development* 137, 1305-14.

Shirayama, M., Seth, M., Lee, H. C., Gu, W., Ishidate, T., Conte, D., Jr. and Mello, C. C. (2012). piRNAs initiate an epigenetic memory of nonself RNA in the C. elegans germline. *Cell* 150, 65-77.

Shukla, A., Yan, J., Pagano, D. J., Dodson, A. E., Fei, Y., Gorham, J., Seidman, J. G., Wickens, M. and Kennedy, S. (2020). poly(UG)-tailed RNAs in genome protection and epigenetic inheritance. *Nature* 582, 283-288.

Sijen, T., Fleenor, J., Simmer, F., Thijssen, K. L., Parrish, S., Timmons, L., Plasterk, R. H. and Fire, A. (2001). On the role of RNA amplification in dsRNA-triggered gene silencing. *Cell* 107, 465-76.

Spike, C. A., Bader, J., Reinke, V. and Strome, S. (2008). DEPS-1 promotes P-granule assembly and RNA interference in C. elegans germ cells. *Development* 135, 983-93.

Strome, S. and Wood, W. B. (1982). Immunofluorescence visualization of germ-line-specific cytoplasmic granules in embryos, larvae, and adults of Caenorhabditis elegans. *Proc. Natl. Acad. Sci. U. S. A.* 79, 1558-62.

Subramaniam, K. and Seydoux, G. (2003). Dedifferentiation of primary spermatocytes into germ cell tumors in C. elegans lacking the pumilio-like protein PUF-8. *Curr. Biol.* 13, 134-9.

Tabara, H., Hill, R. J., Mello, C. C., Priess, J. R. and Kohara, Y. (1999a). pos-1 encodes a cytoplasmic zinc-finger protein essential for germline specification in C. elegans. *Development* 126, 1-11.

Tabara, H., Sarkissian, M., Kelly, W. G., Fleenor, J., Grishok, A., Timmons, L., Fire, A. and Mello, C. C. (1999b). The rde-1 gene, RNA interference, and transposon silencing in C. elegans. *Cell* 99, 123-32.

Thivierge, C., Makil, N., Flamand, M., Vasale, J. J., Mello, C. C., Wohlschlegel, J., Conte, D., Jr. and Duchaine, T. F. (2011). Tudor domain ERI-5 tethers an RNA-dependent RNA polymerase to DCR-1 to potentiate endo-RNAi. *Nat. Struct. Mol. Biol.* 19, 90-7.

Timmons, L., Court, D. L. and Fire, A. (2001). Ingestion of bacterially expressed dsRNAs can produce specific and potent genetic interference in Caenorhabditis elegans. *Gene* 263, 103-12.

Updike, D. and Strome, S. (2010). P granule assembly and function in Caenorhabditis elegans germ cells. *J. Androl.* 31, 53-60.

Vaid, S., Ariz, M., Chaturbedi, A., Kumar, G. A. and Subramaniam, K. (2013). PUF-8 negatively regulates RAS/MAPK signalling to promote differentiation of C. elegans germ cells. *Development* 140, 1645-54.

Voronina, E. and Seydoux, G. (2010). The C. elegans homolog of nucleoporin Nup98 is required for the integrity and function of germline P granules. *Development* 137, 1441-50.

Wan, G., Fields, B. D., Spracklin, G., Shukla, A., Phillips, C. M. and Kennedy, S. (2018). Spatiotemporal regulation of liquid-like condensates in epigenetic inheritance. *Nature* 557, 679-683.

Wickens, M., Bernstein, D. S., Kimble, J. and Parker, R. (2002). A PUF family portrait: 3'UTR regulation as a way of life. *Trends Genet.* 18, 150-7.

Witze, E. S., Field, E. D., Hunt, D. F. and Rothman, J. H. (2009). C. elegans pur alpha, an activator of end-1, synergizes with the Wnt pathway to specify endoderm. *Dev. Biol.* 327, 12-23.

Wolke, U., Jezuit, E. A. and Priess, J. R. (2007). Actin-dependent cytoplasmic streaming in C. elegans oogenesis. *Development* 134, 2227-36.

Yigit, E., Batista, P. J., Bei, Y., Pang, K. M., Chen, C. C., Tolia, N. H., Joshua-Tor, L., Mitani, S., Simard, M. J. and Mello, C. C. (2006). Analysis of the C. elegans Argonaute family reveals that distinct Argonautes act sequentially during RNAi. *Cell* 127, 747-57.

Zetka, M. C., Kawasaki, I., Strome, S. and Muller, F. (1999). Synapsis and chiasma formation in Caenorhabditis elegans require HIM-3, a meiotic chromosome core component that functions in chromosome segregation. *Genes Dev.* 13, 2258-70.

Zhang, Q., Pedigo, N., Shenoy, S., Khalili, K. and Kaetzel, D. M. (2005). Puralpha activates PDGF-A gene transcription via interactions with a G-rich, single-stranded region of the promoter. *Gene* 348, 25-32.

Figures

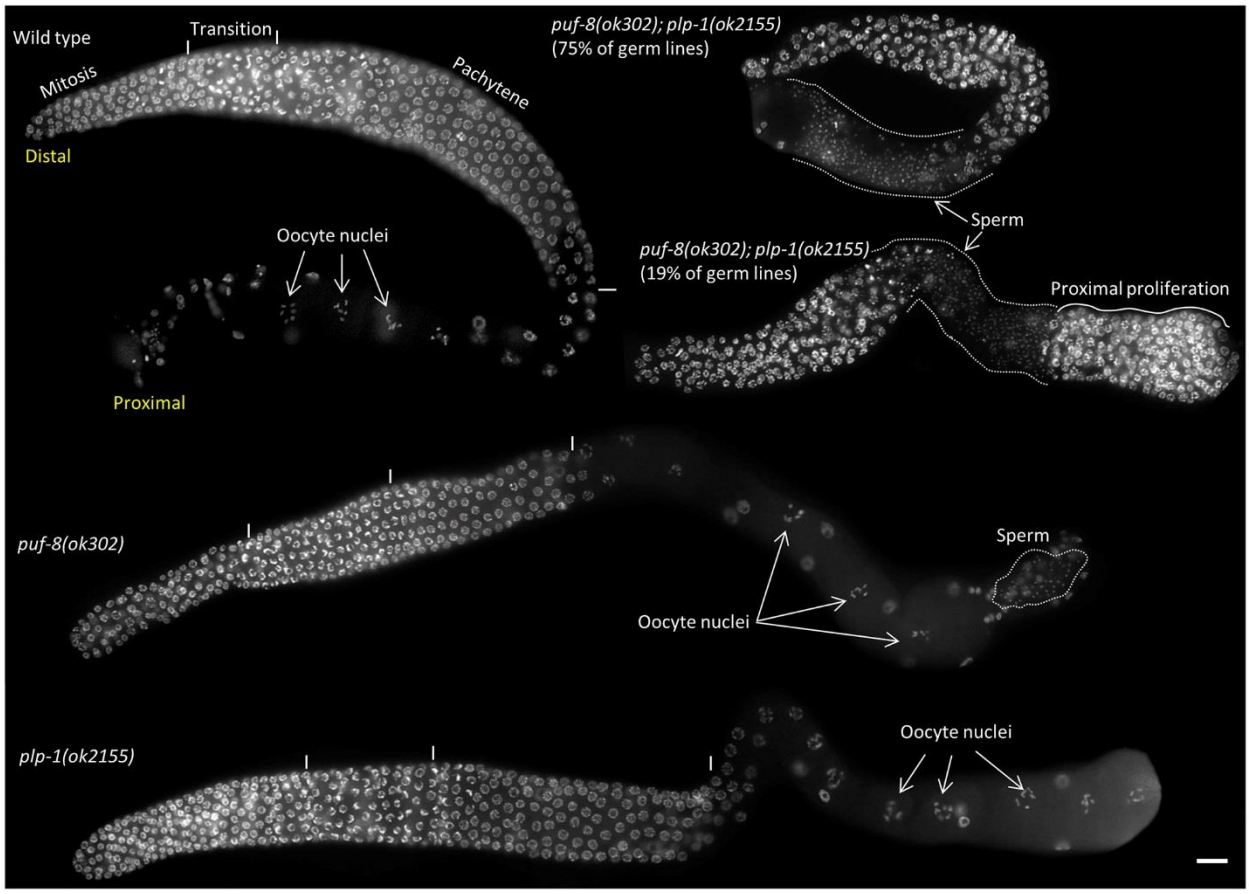

Fig. 1. *puf-8; plp-1* double mutant germ lines do not produce oocytes. Germ lines extruded from 1-day-old adults and stained with DAPI are shown. Approximate boundaries of different developmental stages are indicated by vertical lines and labelled above the wild-type germ line. While oocyte nuclei can be seen in wild-type and the two single mutant germ lines, they are absent in the *puf-8; plp-1* double mutant. The double mutant germ lines are relatively shorter, and the chromatin morphologies characteristic of the different developmental stages are not discernible in them. In some of these double mutant germ lines proliferating germ cells are seen in the proximal region. Scale bar = 20µm.

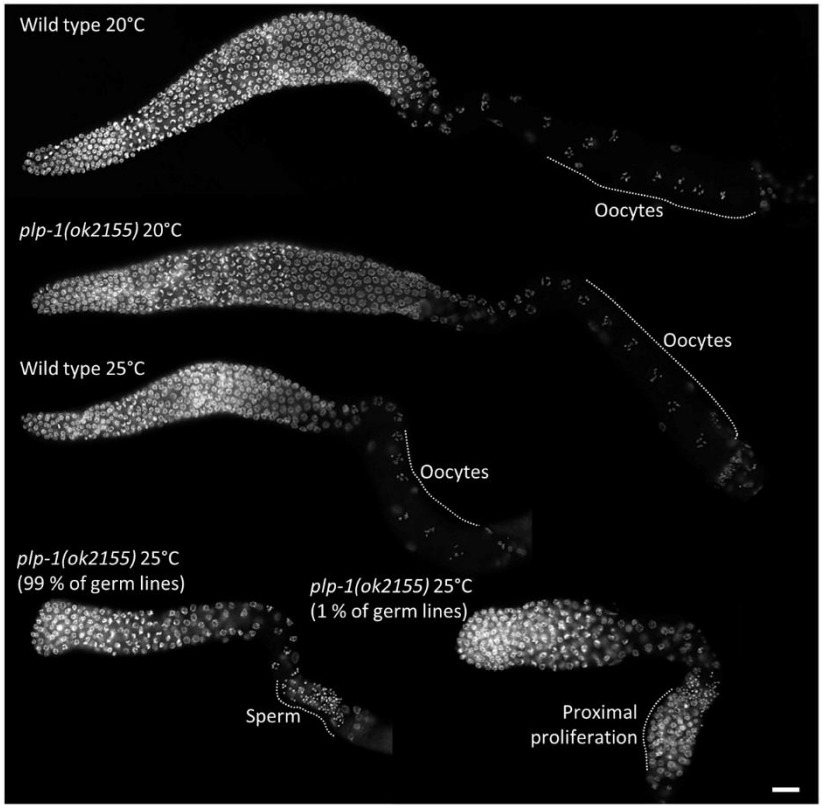

Fig. 2. *plp-1* mutant animals display temperature-sensitive oogenesis defects. Extruded germ lines of wild-type and *plp-1* mutant hermaphrodites grown at the indicated temperatures were stained with DAPI. Similar to the *puf-8; plp-1* double mutant **(Fig. 1)**, *plp-1* single mutants grown at 25°C do not produce oocytes, and some of them develop proximal tumors. Scale bar = 20µm.

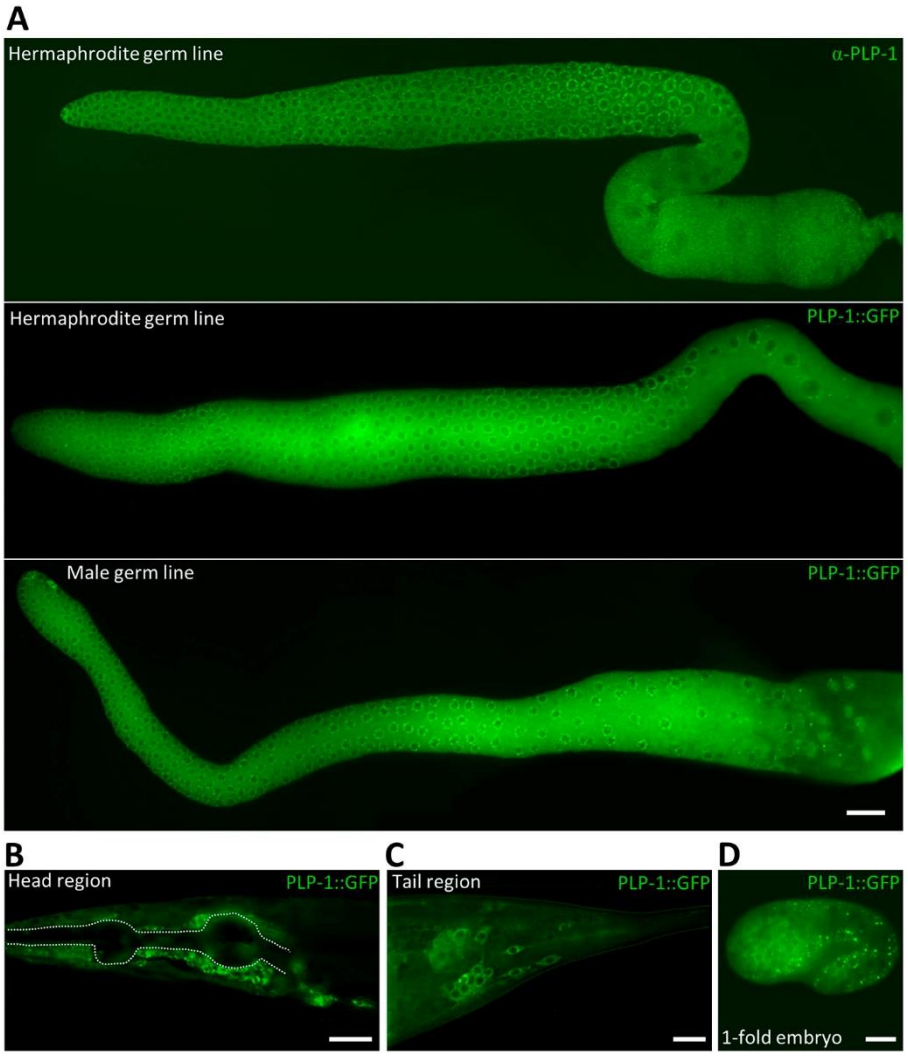

Fig. 3. Distribution patterns of PLP-1. **(A)** Extruded germ lines are shown. **Top** – hermaphrodite germ line fixed and immunostained with anti-PLP-1 antibodies. **Middle** –germ line from a live hermaphrodite carrying the *Pplp-1* ::*plp-1*::*gfp*::*plp-1* 3′ UTR transgene. **Bottom** – germline from a live male carrying the same transgene as above. PLP-1::GFP in the core cytoplasm is noticeable in the transgenic germ lines, while the perinuclear puncta of PLP-1 / PLP-1::GFP are visible in all three. **(B-D)** PLP-1::GFP is expressed in somatic cells around pharynx **(B)**, tail region **(C)** and late-stage embryo **(D)**. Perinuclear PLP-1::GFP puncta are seen in some of these somatic cells as well. Scale bars = 20µm **(A)** and **(B)**, and 10µm **(C)** and **(D)**.

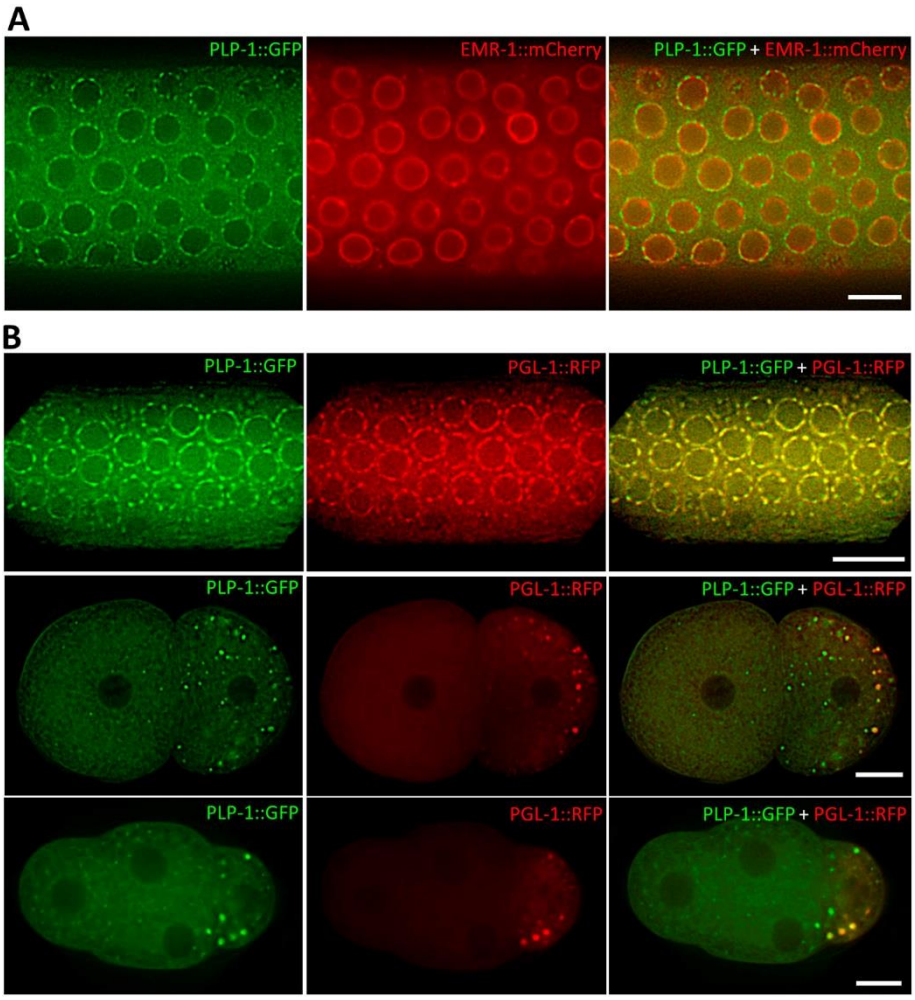

Fig. 4. PLP-1 localizes to perinuclear P granules in the germ line and to P granules and unknown granules in embryos. **(A)** A section of germ line from a hermaphrodite showing the expression of PLP-1::GFP and the nuclear envelope marker EMR-1::mCherry. These fusion proteins are expressed by the transgenes *Pplp-1*::*plp-1*::*gfp*::*plp-1* 3′ UTR and *Ppie-1*::m*Cherry*::*emr-1*::*hip-1* 3′ UTR, respectively. As can been seen in the merged image on the right, the PLP-1::GFP puncta surround the nuclear membrane, indicating that these puncta are cytoplasmic. **(B)** PLP-1::GFP and the P granule marker PGL-1::RFP colocalize in the germ line **(top)** and in 2-cell **(middle)** and 4-cell embryos **(bottom)**. Note: Not all PLP-1::GFP puncta colocalize with the P granules in embryos, and a few smaller and fainter PLP-1::GFP granules are visible in the somatic blastomeres as well. Scale bar = 10µm (all panels).

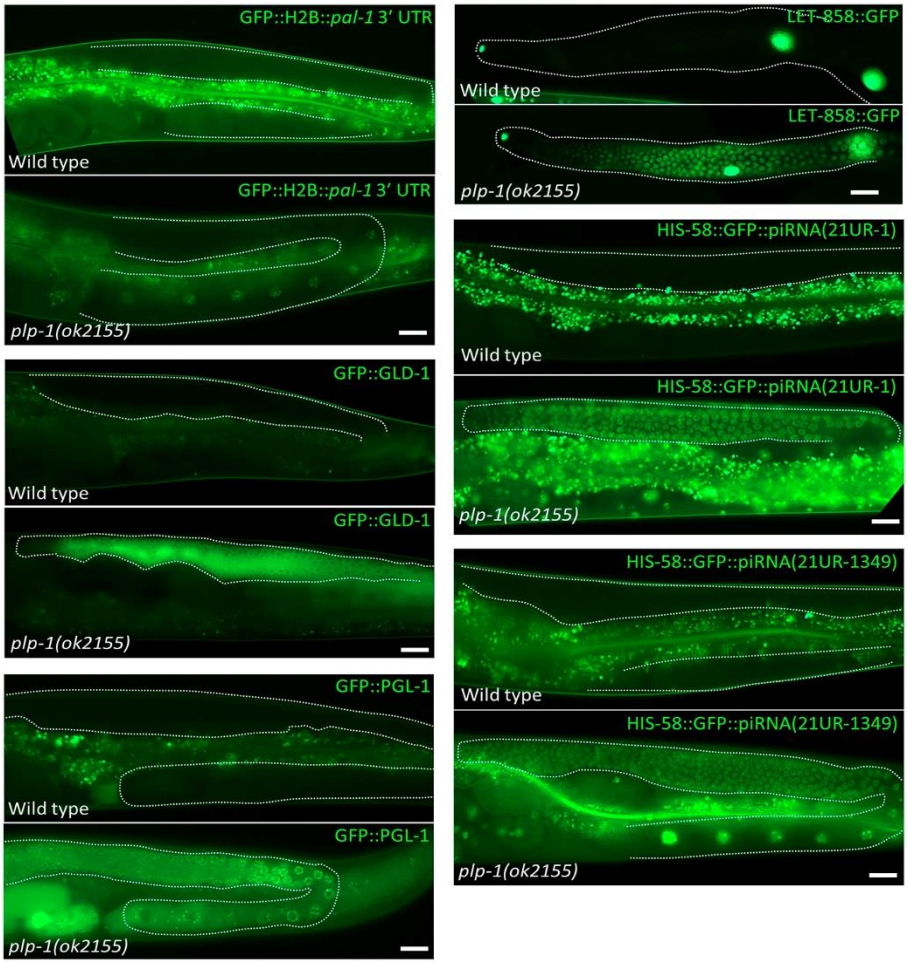

Fig. 5. Integrated and extrachromosomal array transgenes, and piRNA sensors are not silenced in *plp-1* germ lines. GFP fluorescence images of live wild-type and *plp-1(ok2155)* hermaphrodites are shown. GFP::H2B::*pal-1* 3′ UTR, GFP::GLD-1 and GFP::PGL-1 are expressed by integrated, single-copy transgenes (**left**). LET-858::GFP is expressed by the extrachromosomal array *ccEx7271* carrying the *let-858::gfp* transgene; in these extruded germ lines, GFP fluorescence can be seen in three somatic nuclei—the distal tip cell nucleus at the extreme left and two other larger nuclei at the right—in both genotypes, while it is visible in germline nuclei only in the *plp-1* mutant (**right, top**). Expression of HIS-58, which is a histone H2B, fused to GFP by integrated transgenes containing the target sequences of piRNA(21UR-1) (**right, middle**) or piRNA(21UR-1349) (**right, bottom**) in the 3′ UTR. The germ line is outlined (dotted white lines) in all images. Non-specific autofluorescence of gut granules is seen in some images. Scale bar = 20μm.

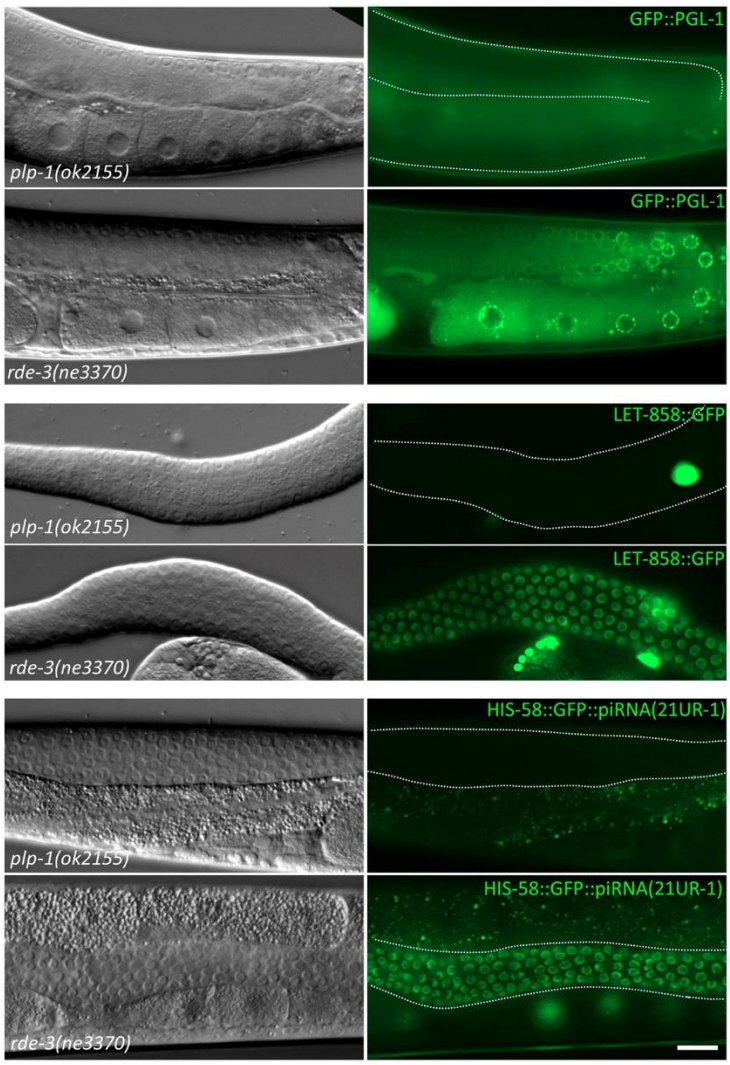

Fig. 6. Already silenced transgenes are not activated in *plp-1* mutants. GFP fluorescence and the corresponding differential interference contrast images of the indicated genotypes are shown. Only part of the germ line, outlined by dotted white lines, is visible in all images. Already silenced *gfp::pgl-1* transgene, c*cEx7271* extrachromosomal array and piRNA sensor-1 are not expressed when introduced into *plp-1*germ lines, but are activated in *rde-3* germ lines. Scale bar = 20µm.

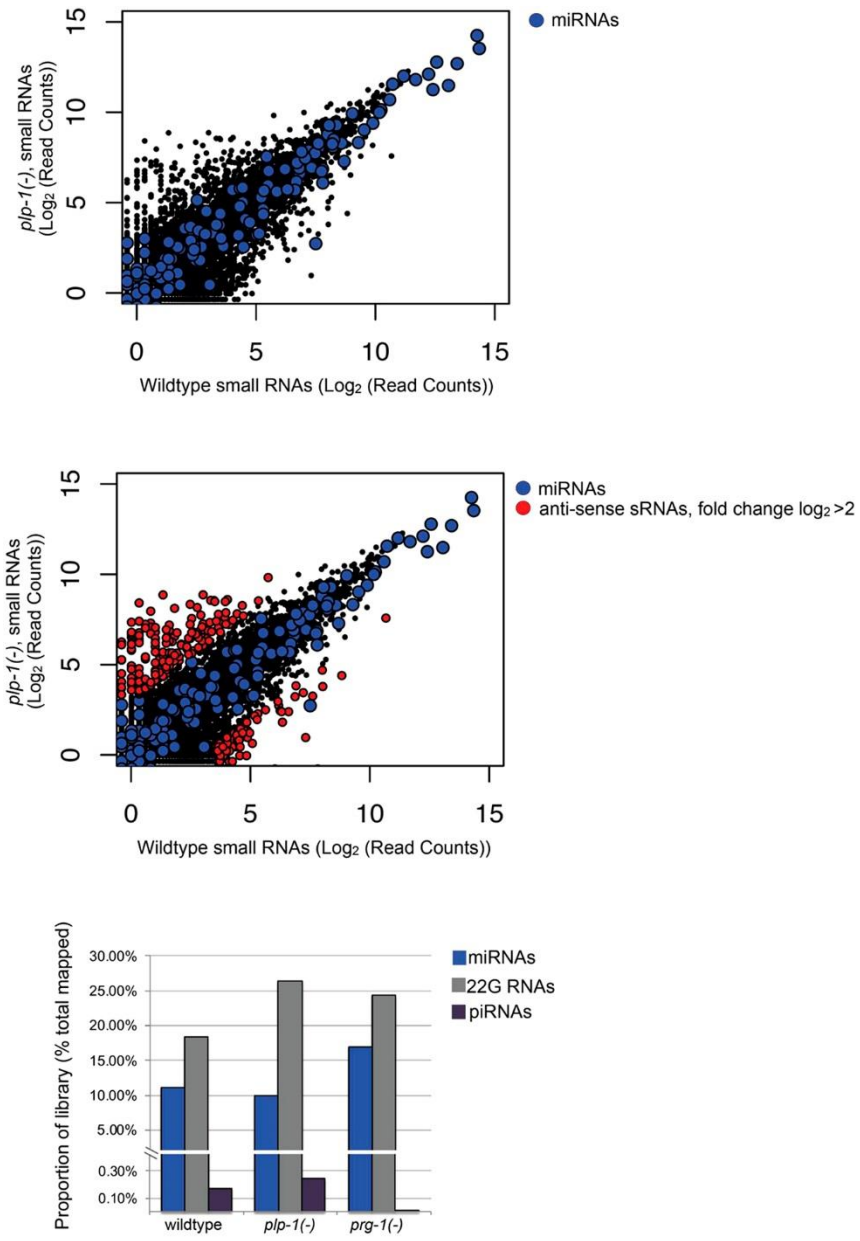

Fig. 7. Biogenesis of small RNAs is not significantly affected in *plp-1* mutants. Top: Small antisense RNA expression in young adult wild-type and *plp-1 (-)* animals. Counts are normalized to total RNAs that aligned to the ce11 genome. miRNA counts are overlaid in blue. **Middle**: Small antisense RNA expression in young adult wild-type and *plp-1 (-)* animals. Counts are normalized to total RNAs that aligned to the ce11 genome. miRNA counts are overlaid in blue. Red-colored dots indicate protein-coding genes with at least 50-mapped reads and 4-fold more or less reads in *plp-1(-)* relative to wild type (212 and 76 genes, respectively).

Bottom: Bar graph indicates the proportion of total library that are miRNAs, 22G antisense small RNAs, and annotated piRNAs. Counts are normalized to total RNAs that aligned to the ce11 genome. See Materials and methods, and Supplementary dataset-1 for more details.

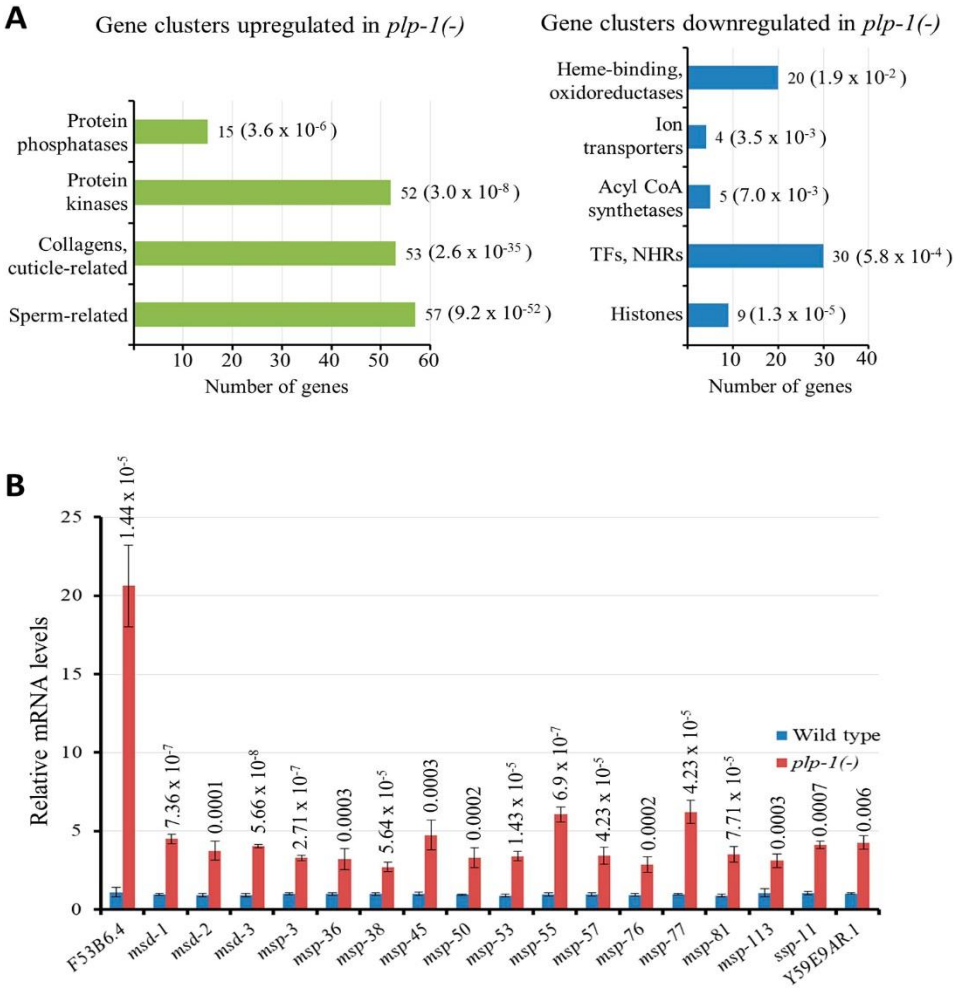

Fig. 8. Sperm-related and, collagen and other cuticle-related genes are significantly upregulated in *plp-1* mutants. **(A)** Bar graphs shown here compare the groups of genes whose mRNA levels are significantly higher **(left)** or lower **(right)** in *plp-1*mutants than in wild type. The *p*-values for the enrichment are indicated in parentheses. The lists of genes are presented in Supplementary dataset-3 and -4. The mRNA levels were measured using high throughput, transcriptome sequencing. Total processed and mapped reads ranged from 43,557,204 to 60,518,575 among the six samples (three biological replicates each of *plp-1(-)* and wild type). See Materials and methods, and Supplementary dataset-2 for more details. **(B)** Validation of the sequencing results. Transcript levels of 18 sperm-related genes, which were identified as upregulated by transcriptome sequencing, were quantitated using quantitative RT-PCR. Error bars represent standard deviation. The *p*-values, indicated above the bars, were calculated by Student's t-test.

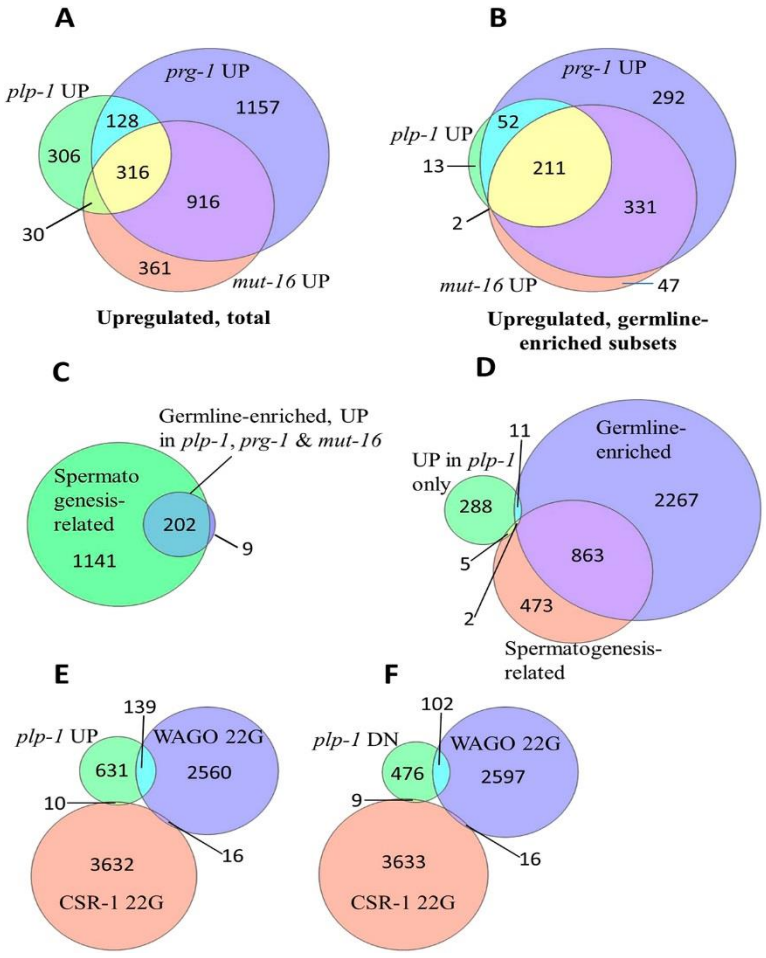

Fig. 9. Meta-analysis of transcriptome datasets. Proportional Venn diagram representations show **(A)** significant overlap of genes upregulated in *plp-1*, *prg-1* and *mut-16* mutants (*p*-values: < 8.8 x 10^{-203} for the overlap between *plp-1* and *prg-1*, and < 9.6 x 10^{-176} for *plp-1* and *mut-16*). **(B)** The overlap is substantially higher among the upregulated genes that are more abundantly expressed in the germ line (germline-enriched). **(C)** Spermatogenesis-related genes dominate (95 %) among germline-enriched genes that are upregulated in all three mutants. **(D)** Majority of genes upregulated only in *plp-1* are non-germline-enriched. **(E, F)** While targets of WAGO-class 22G-RNAs are essentially equally represented in both *plp-1(-)*-upregulated and *plp-1(-)*-downregulated groups, targets of CSR-1-22G-RNAs are almost excluded from these two groups. See supplementary dataset-2 for lists of genes represented in the Venn diagrams shown here. *prg-1* and m*ut-16* datasets are from (Reed et al., 2020); germline-enriched and spermatogenesis-related datasets are from (Reinke et al., 2004); and lists of targets of WAGO- and CSR-1-22G-RNAs are from (Lee et al., 2012).

Supplemental material

PLP-1 is essential for germ cell development and germline gene silencing in *C. elegans*

Rajaram Vishnupriya, Linitha Thomas, Lamia Wahba, Andrew Fire and Kuppuswamy Subramaniam

Figure S1

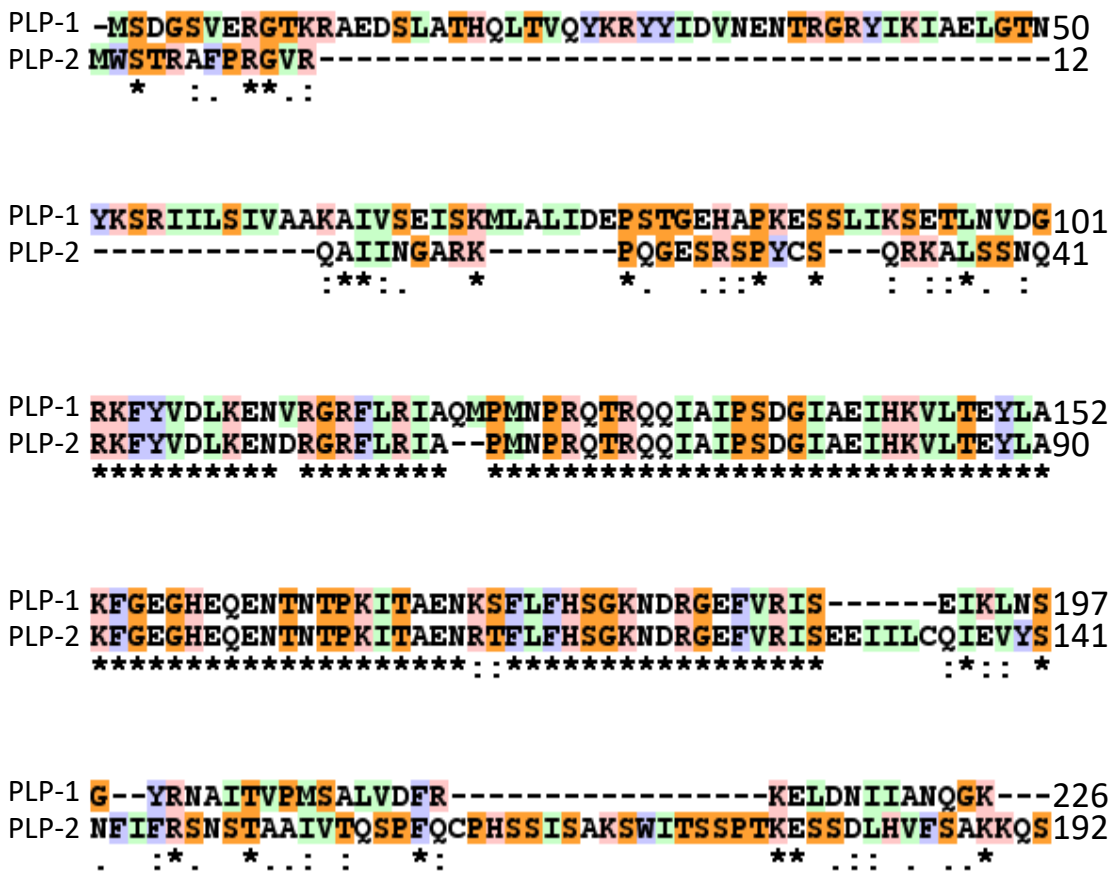

Fig. S1. Alignment of the amino acid sequences of PLP-1 and PLP-2. Amino acid sequences have been aligned using the CLUSTALW program supplied with the DNA DYNAMO software package. GenBank accession numbers: PLP-1 – NP_501241; PLP-2 – CAB01747. Identical amino acids are indicated by an asterisk (*), and the ones with very similar side chains and somewhat similar sides chains are indicated by two dots (:) and by single dot (.), respectively.

Figure S2

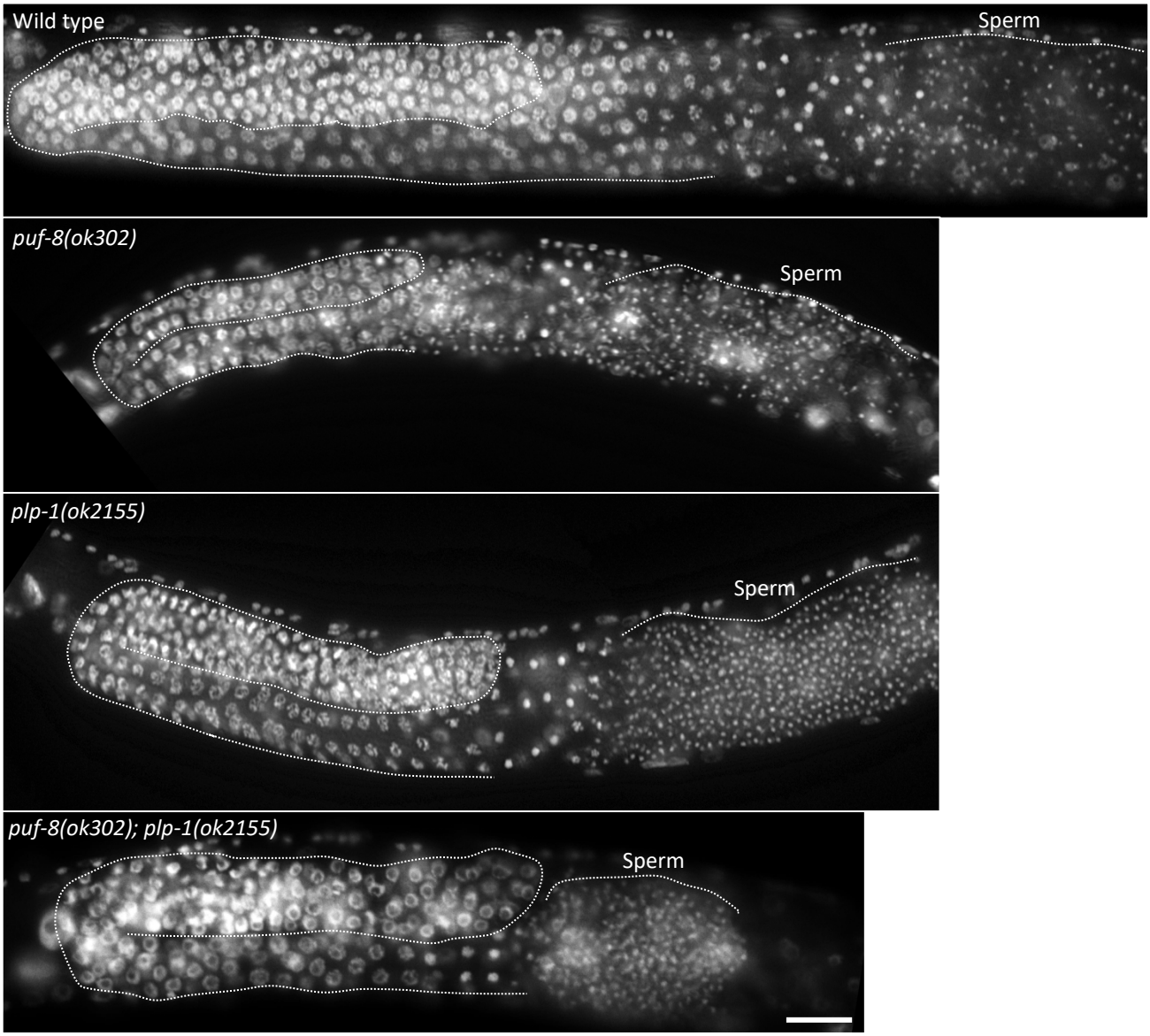

Fig. S2. PUF-8 and PLP-1 are not essential for spermatogenesis in males. Adult males of the indicated genotypes stained with DAPI are shown. Scale bar = 20µm.

Figure S3

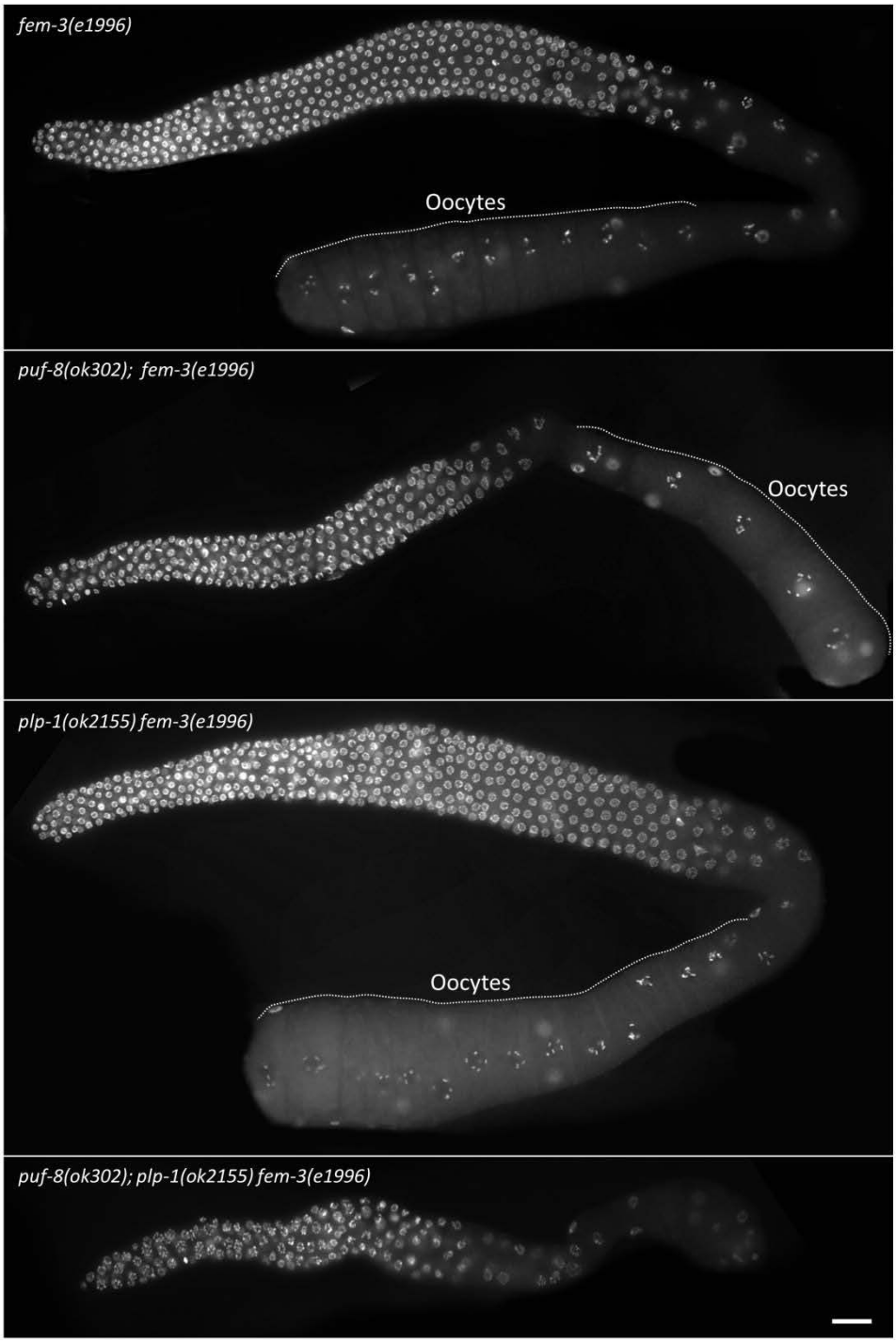

Fig. S3. Germ lines missing PUF-8 and PLP-1 fail to produce oocytes. Extruded germ lines of the indicated genotypes stained with DAPI are shown. The *puf-8; plp-1* mutant germ lines do not produce oocytes even when set in the "female mode" by the *fem-3* mutation. Scale bar = 20µm.

Figure S4

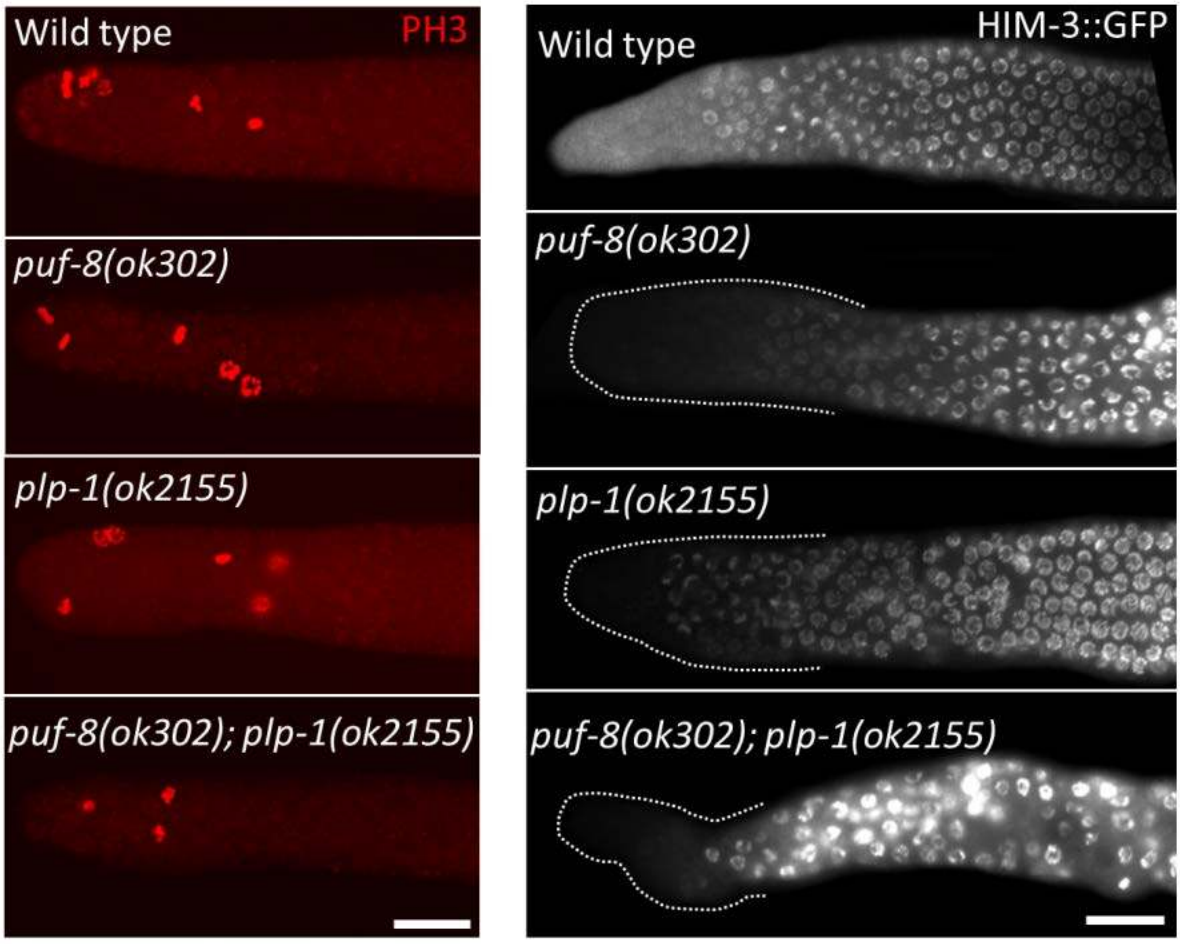

Fig. S4. Mitotic proliferation and meiotic entry are not affected in *puf-8; plp-1* germ lines. **Left** – Extruded germ lines of the indicated genotypes immunostained with anti-phosphohistone H3 (PH3) antibodies are shown. Metaphase nuclei brightly stained with anti-PH3 antibodies are visible in all genotypes. Average numbers of PH3-positive nuclei per germ line were: wild type –4.82 (n=71); *puf-8* – 3.02 (n=46); *plp-1* – 4.33 (n=67) and *puf-8; plp-1* – 1.77 (30). Right – Germ lines extruded from live worms carrying the *him-3::gfp* transgene are shown. Expression of the meiotic marker HIM-3::GFP is seen in all genotypes. Scale bar = 20µm.

Figure S5

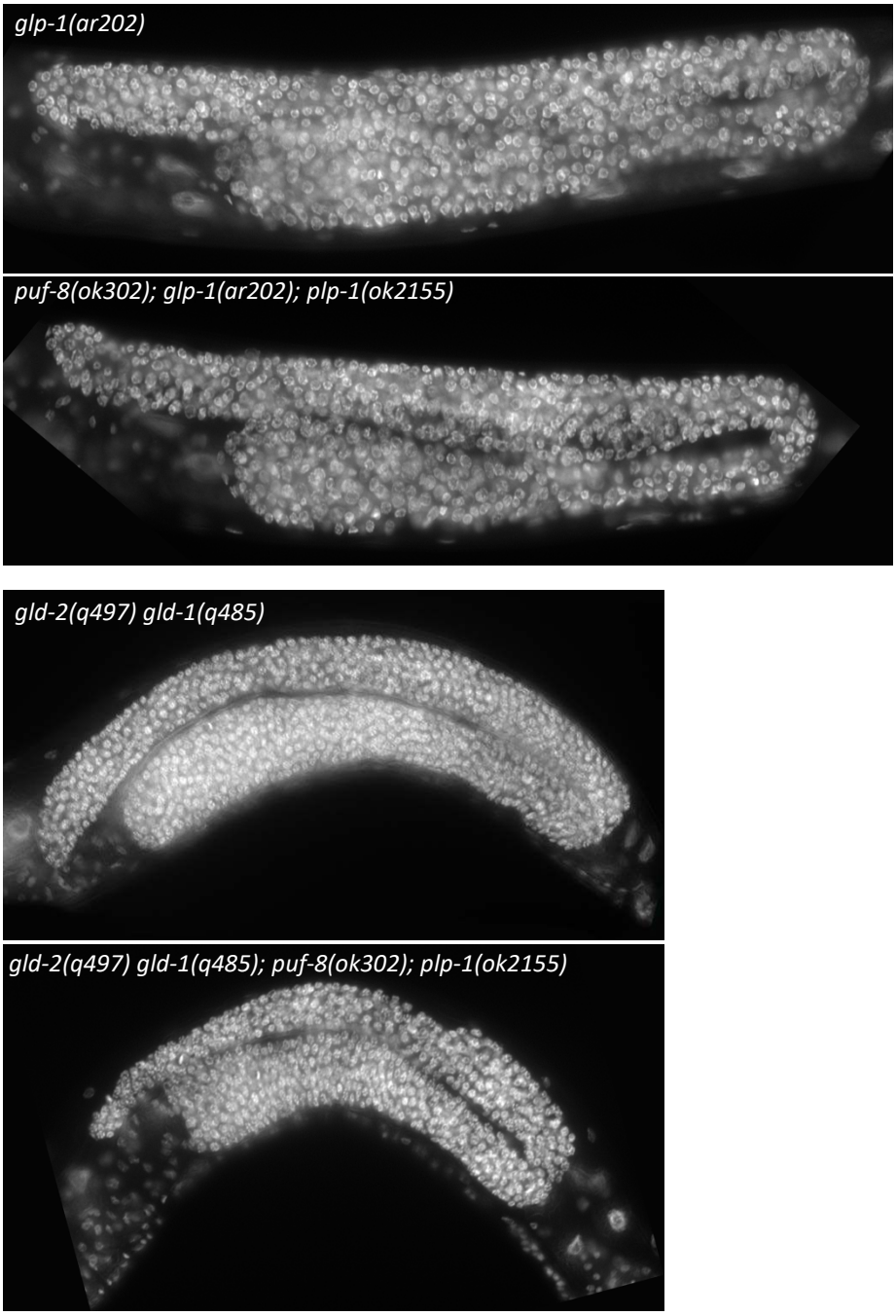

Fig. S5. PUF-8 and PLP-1 are not essential for tumor development in germ lines defective for meiotic entry. DAPI-stained animals of the indicated genotypes are shown. Only parts of animals revealing one of the gonadal arms are shown.

Figure S6

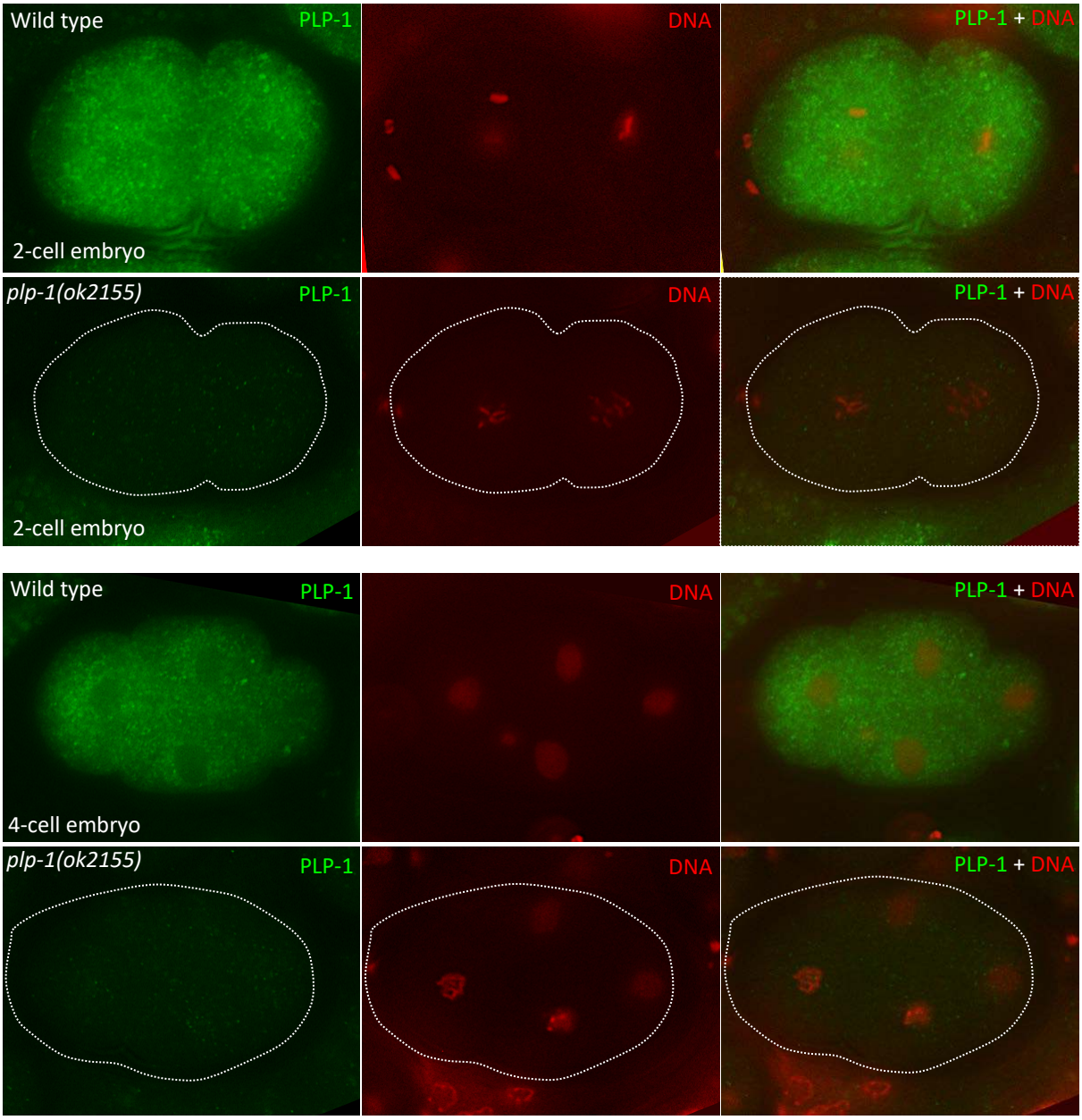

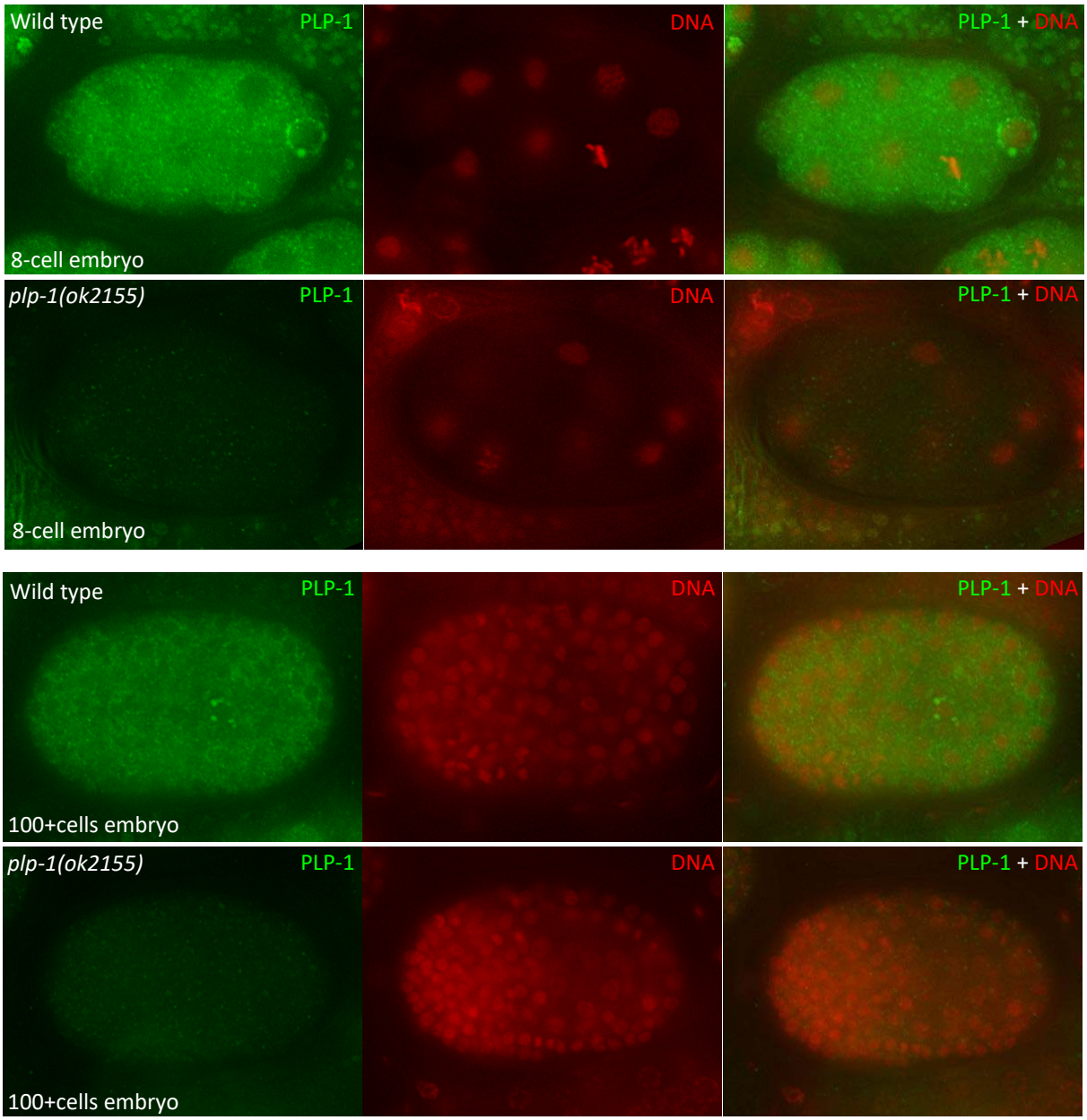

Fig. S6. PLP-1 is present in all blastomeres throughout embryo development. Embryos at different stages of development were stained with anti-PLP-1 antibodies (green) and DAPI (red). Immunofluorescence signals could be detected in the cytoplasm of all blastomeres throughout embryonic development in wild-type embryos. By contrast, no immunofluorescence was detected in *plp-1* mutant embryos, indicating that the antibody is PLP-1-specific. Perinuclear PLP-1 puncta are visible in the 8-cell (near the right end of the embryo) and 100+cells (middle right of the embryo) wild-type embryos. These puncta are not prominent in younger embryos, presumably due to the effect of formaldehyde fixation.

Figure S7

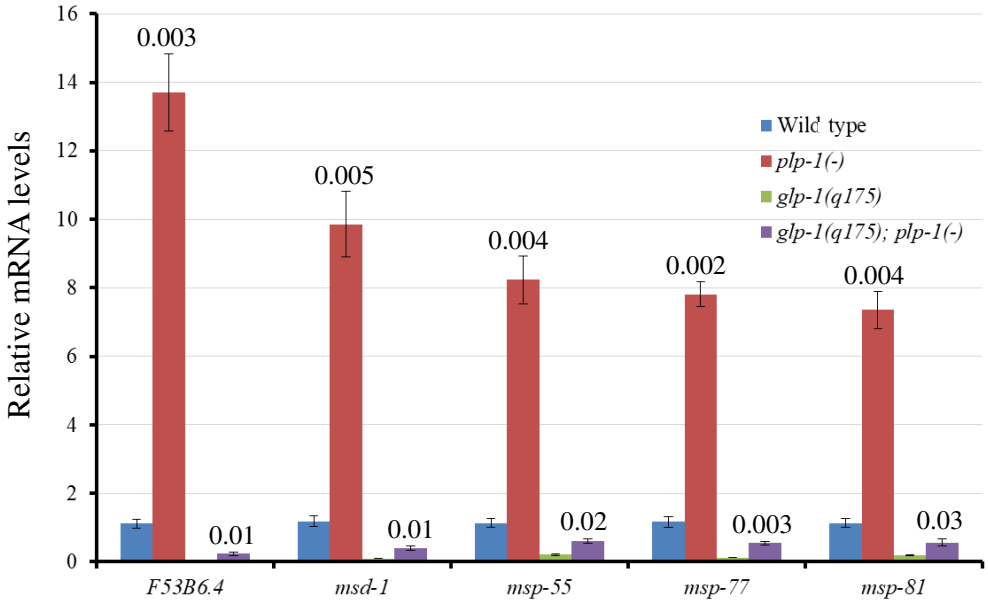

Fig. S7. PLP-1 negatively regulates the expression of sperm-related genes in the germ line. Transcript levels, quantitated by quantitative RT-PCR, of five sperm-related genes in adult hermaphrodites of the indicated genotypes are shown. All values are relative to the wild-type level which is taken as 1. These five genes were randomly selected from the list of genes identified by transcriptome sequencing as upregulated in *plp-1* mutants. Very low levels in *glp-1(q175)*, which lacks germ cells, show that these genes are mainly expressed in the germ line. Increase in transcript levels in the germ line is largely responsible for the upregulation seen in *plp-1* single mutants (compare red and purple bars). Error bars represent standard deviation. Numbers above the bars are *p*-values calculated using Student's t-test.

Figure S8

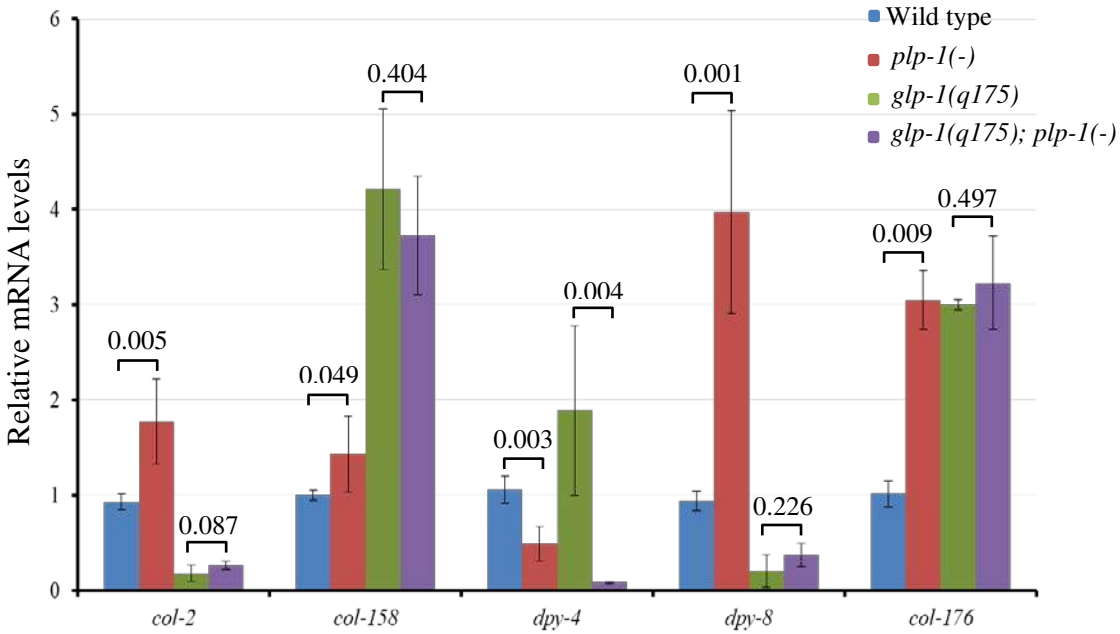

Fig. S8. Loss of PLP-1 results in the misexpression of some non-germline-enriched genes in the germ line. Transcript levels, quantitated by quantitative RT-PCR, of five non-germline-enriched genes in adult hermaphrodites of the indicated genotypes are shown. All values are relative to the wild-type level which is taken as 1. These five genes were randomly selected from the list of genes identified by transcriptome sequencing as upregulated in *plp-1* mutants. Difference between wild type and *glp-1(q175)*, which lacks germ cells, represents the level of expression in the germ line. In the absence of PLP-1, *col-2* and *dpy-8* transcript levels increase in the germ line (compare the differences between blue and red bars with green and purple bars). Intriguingly, *col-158* and *col-176* levels increase in *glp-1(q175)* animals; whether the absence of germ cells or GLP-1 led to this increase is not clear. In contrast to the transcriptome-sequencing results, qRT-PCR indicates a decrease in the transcript levels of *dpy-4* in *plp-1* mutant animals. Error bars represent standard deviation. Numbers above the bars are *p*-values calculated using Student's t-test.

Figure S9

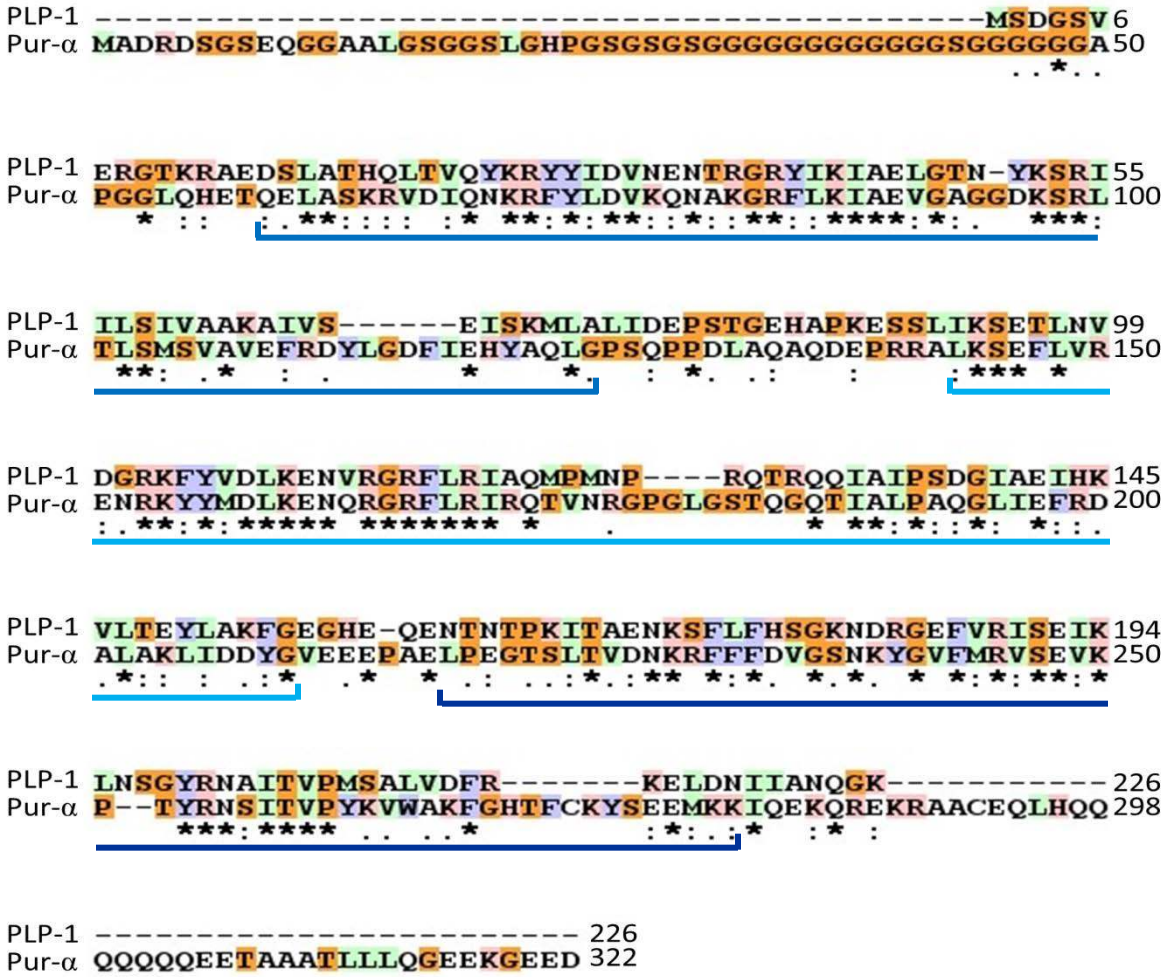

Fig. S9. Alignment of the amino acid sequences of *C. elegans* PLP-1 and human Pur-alpha proteins. The three Pur repeats are underlined. GenBank accession numbers: PLP-1 – NP_501241; human Pur-alpha – AAV38195. Identical amino acids are indicated by an asterisk (*), and the ones with very similar side chains and somewhat similar sides chains are indicated by two dots (:) and by single dot (.), respectively.

Figure S10

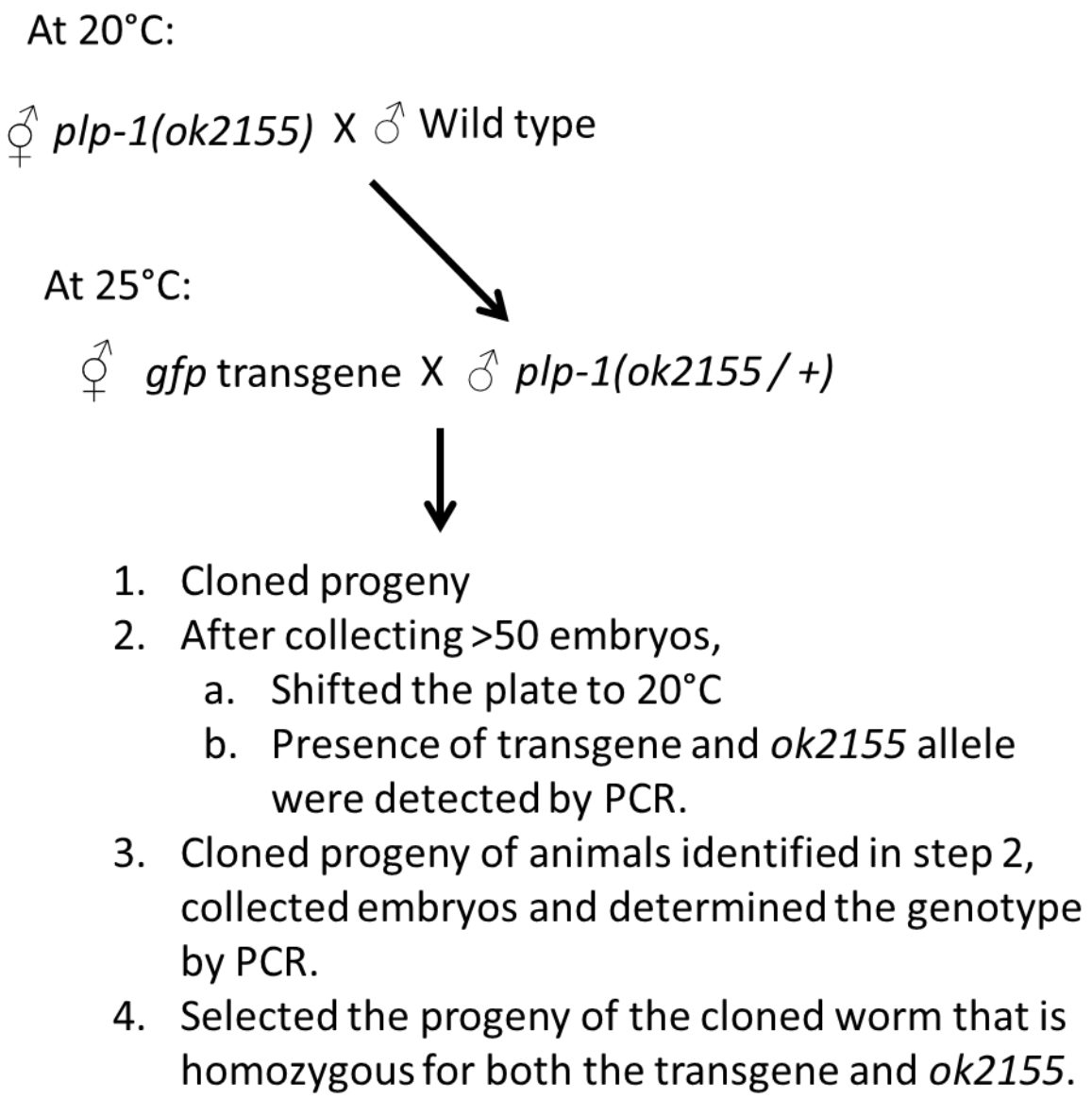

Fig. S10. Flowchart illustration of the scheme for introducing silencing-prone transgenes into the *plp-1* mutant background

Table S1. Genetic redundancy between *puf-8* and *plp-1* in the germ line

Genotype	Percent of fertile worms (n)	Percent of sterile worms (n)
Wild type	100 (500)	0 (500)
puf-8(ok302)	100 (548)	0 (548)
plp-1(ok2155)	100 (500)	0 (500)
puf-8(ok302); plp-1(ok2155)	0.56 (358)	99.44 (358)

Table S2. *plp-1(-)* hermaphrodites are sterile at 25°C

Genotype	Percent of fertile worms (n)	Percent of sterile worms (n)	Percent of worms with endomitotic oocytes (n)
Wild type 1-day-old adults	100 (114)	0 (114)	0 (114)
plp-1(ok2155) 1-day-old adults	0 (248)	100 (248)	0 (248)
plp-1(ok2155) 2-day-old adults	0 (162)	100 (162)	63 (162)
plp-1(ok2155) 3-day-old adults	0 (68)	100 (68)	Not determined

Table S3. Summary of the observations from the single-male crosses

Plate No.	Progeny present?	Genotype of the male parent	Plate No.	Progeny present?	Genotype of the male parent
1	Yes	*plp-1(-/+)*	13	No	***plp-1(-/-)***
2	Yes	*plp-1(-/+)*	14	No	***plp-1(-/-)***
3	Yes	*plp-1(-/+)*	15	No	***plp-1(-/-)***
4	Yes	*plp-1(-/+)*	16	No	*plp-1(-/+)*
5	Yes	*plp-1(-/+)*	17	No	***plp-1(-/-)***
6	Yes	*plp-1(-/+)*	18	No	*plp-1(-/+)*
7	Yes	*plp-1(-/+)*	19	No	***plp-1(-/-)***
8	Yes	*plp-1(-/+)*	20	No	***plp-1(-/-)***
9	Yes	*plp-1(-/+)*	21	No	***plp-1(-/-)***
10	Yes	*plp-1(-/+)*	22	No	***plp-1(-/-)***
11	Yes	*plp-1(-/+)*	23	No	*plp-1(-/+)*
12	Yes	*plp-1(-/+)*	24	No	*plp-1(-/+)*

Table S4. Response of *plp-1(ok2155)* mutants to RNAi

	Percent of viable embryos (n)	
Target of RNAi	**Wild type**	***plp-1(ok2155)***
mex-3	0.49 (1843)	0.31 (1287)
pos-1	1.21 (1901)	11.77 (1368)
spn-4	1.38 (1805)	15.41 (1590)
Non-RNAi control	100 (1110)	99.68 (1248)

Table S5. List of *C. elegans* strains used in this study

Click here to Download Table S5

Table S6. List of oligonucleotides used in this study

Click here to Download Table S6

Supplementary Data S1

Click here to Download Data S1

Supplementary Data S2

Click here to Download Data S2

Supplementary Data S3

Click here to Download Data S3

Supplementary references

Ariz, M. (2010). Identifying partners of PUF-8, a *C. elegans* member of the PUF family of RNA-binding proteins, *PhD thesis*, Indian Institute of Technology, Kanpur, India.

Bagijn, M. P., Goldstein, L. D., Sapetschnig, A., Weick, E. M., Bouasker, S., Lehrbach, N. J., Simard, M. J. and Miska, E. A. (2012). Function, targets, and evolution of Caenorhabditis elegans piRNAs. *Science* 337, 574-578.

Cheeks, R. J., Canman, J. C., Gabriel, W. N., Meyer, N., Strome, S. and Goldstein, B. (2004). C. elegans PAR proteins function by mobilizing and stabilizing asymmetrically localized protein complexes. *Curr. Biol*. 4, 851-62.

Kelly, W. G., Xu, S., Montgomery, M. K. and Fire, A. (1997). Distinct requirements for somatic and germline expression of a generally expressed Caernorhabditis elegans gene. *Genetics* 146, 227-38.

Merritt, C., Rasoloson, D., Ko, D. and Seydoux, G. (2008). 3' UTRs are the primary regulators of gene expression in the C. elegans germline. *Curr. Biol.* 18, 1476-82.

Pepper, A. S., Killian, D. J. and Hubbard, E. J. (2003). Genetic analysis of Caenorhabditis elegans glp-1 mutants suggests receptor interaction or competition. *Genetics* 163, 115-32.

Pushpa, K., Kumar, G. A. and Subramaniam, K. (2013). PUF-8 and TCER-1 are essential for normal levels of multiple mRNAs in the C. elegans germline. *Development* 140, 1312-20.

Shirayama, M., Seth, M., Lee, H. C., Gu, W., Ishidate, T., Conte, D., Jr. and Mello, C. C. (2012). piRNAs initiate an epigenetic memory of nonself RNA in the C. elegans germline. *Cell* 150, 65-77.

Subramaniam, K. and Seydoux, G. (2003). Dedifferentiation of primary spermatocytes into germ cell tumors in C. elegans lacking the pumilio-like protein PUF-8. *Curr. Biol.* 13, 134-9.

Tabara, H., Sarkissian, M., Kelly, W. G., Fleenor, J., Grishok, A., Timmons, L., Fire, A. and Mello, C. C. (1999). The rde-1 gene, RNA interference, and transposon silencing in C. elegans. *Cell* 99, 123-32.

Wolke, U., Jezuit, E. A. and Priess, J. R. (2007). Actin-dependent cytoplasmic streaming in C. elegans oogenesis. *Development* 134, 2227-36.